Levels of Si^{29} with Excitation Energy Below 6.4 MeV*

T. T. Bardin, J. A. Becker, T. R. Fisher, and A. D. W. Jones†
Lockheed Palo Alto Research Laboratory, Palo Alto, California 94304
(Received 28 May 1971)

Levels in Si^{29} were populated with the reaction $Mg^{26}(\alpha, n)Si^{29}$ and subsequent γ radiation from the various levels was detected with a 37-cm^3 Ge(Li) γ-ray spectrometer. Beginning with the 4.08-MeV level, γ-ray angular distributions ($0° \leq \theta_\gamma \leq 90°$) were measured at incident bombarding energies near threshold ($Q_0 = 0.033$ MeV) for levels with excitation energies between 4.08 and 6.38 MeV. The target was a Mg^{26} metal foil, on the order of 0.5 mg/cm^2 thickness. Branching ratios and excitation energies of the various levels were deduced from γ-ray pulse-height distributions. γ-ray angular correlations obtained at α bombarding energies near threshold were treated as originating from residual nuclei having magnetic quantum numbers $|m| = \frac{1}{2}$ and $\frac{3}{2}$. Analysis of these angular correlations in terms of level spin and γ-ray multipole mixing was then undertaken. Mean lifetimes (or limits) for these levels were determined using a variant of the Doppler-shift-attenuation method, which involves measurements of the attenuation for two targets of different stopping power. Both Mg^{26} foils and Mg^{26}-Au alloy foils (10 at.% Mg^{26} and 90 at.% Au) were used. From these measurements, excitation energies (in keV), level spins, and lifetimes (in fsec) for these levels were deduced; these are, respectively, 4079.5 ± 0.4, $\frac{7}{2}$, 48 ± 8; 4740.5 ± 0.4, $\frac{5}{2}$ or $\frac{9}{2}$, 45 ± 10; 4838.5 ± 0.8, $\frac{1}{2}$ or $\frac{3}{2}$, <5; 4894.9 ± 0.6, $\frac{5}{2}$, 10 ± 3; 4932.6 ± 0.4, $\frac{3}{2}$, <10; 5254.1 ± 0.5, $\frac{9}{2}$, 100 ± 20; 5284.4 ± 0.7, $\frac{3}{2}$ or $\frac{7}{2}$, <10; 5651.8 ± 0.7, $\frac{5}{2}$ or $\frac{9}{2}$, 40 ± 15; 5810.7 ± 1.2, $\frac{7}{2}$, <20; 5946.3 ± 3.0, $\frac{3}{2}$, <30; 6106.6 ± 0.6, $\frac{3}{2}$ or $\frac{5}{2}$, <8; 6190.7 ± 1.3, $\frac{3}{2}$, $\frac{5}{2}$, or $\frac{7}{2}$, <15; 6378.8 ± 3.0, $\frac{1}{2}$ or $\frac{3}{2}$. Excitation energies and lifetimes of levels with $E_x < 4.08$ were determined as well. These are (keV, fsec) 1273.1 ± 0.2, 360 ± 70; 2027.6 ± 0.2, 360 ± 70; 2425.0 ± 0.4, 13 ± 3; 3066.9 ± 0.5, 20 ± 7; 3623.1 ± 0.3, 4000 ± 800. These data may be combined with the results of other investigations to arrive at a fairly complete level scheme for Si^{29} in the energy interval $0 < E_x$ (Mev) < 6.38, including a description of the electromagnetic decay properties. These properties are compared with model predictions of the properties of Si^{29}.

I. INTRODUCTION

The nucleus Si^{29} lies in the mass region of the nuclear $2s$-$1d$ shell where the nuclear deformation is changing from prolate to oblate. In terms of the unified nuclear model[1,2] the coupling between the collective and individual particle motions is not clear, i.e., whether the weak- or strong-coupling approach provides the best description. Both approaches have been used in calculations.[3-6] There have not been any extensive "microscopic" shell-model studies made, because of the complexity of the problem. Furthermore, it would seem clear that it is easy to excite particles from the Si^{28} core, and so shell-model interpretations of Si^{29} will not be especially simple.

Historically, Si^{29} was one of the first light nuclei after Al^{25} to be interpreted from the point of view of the collective model. Although experimental information was scanty, e.g., level spins and decay modes were known only for the states with $E_x \leq 3.62$ MeV, Bromley, Gove, and Litherland[5] concluded that properties of the low-lying levels could best be described by the strong-coupling model of Nilsson,[2] and that the nucleus was characterized by an (oblate) deformation $\eta = -2$. In this interpretation the states at 0, 2.426, and 2.028 MeV are described as the $J^\pi = \frac{1}{2}^+$, $\frac{3}{2}^+$, and $\frac{5}{2}^+$ members of the $K^\pi = \frac{1}{2}^+$ band based on a neutron in Nilsson orbit No. 9, while the states at 1.273 and 3.069 MeV are interpreted as the $J^\pi = \frac{3}{2}^+$ and $\frac{5}{2}^+$ members of a $K^\pi = \frac{3}{2}^+$ band based on a neutron in orbit No. 8. This picture did not describe the electromagnetic decay properties of these levels very well[7]; however Hirko[6] has shown that when these bands (the $K^\pi = \frac{1}{2}^+$ and $K^\pi = \frac{3}{2}^+$ bands from Nilsson orbits 9 and 8, respectively) are allowed to mix, good agreement is obtained with the electromagnetic decays. Recently, Jones *et al.*,[8] based on their study of the $Al^{29}(\beta^-)Si^{29}$ decay, have concluded that the situation is more complicated than this. They postulate an unmixed $K^\pi = \frac{5}{2}^+$ wave function for the ground state of Al^{29}, based on a proton in orbit No. 5, and find that successful treatment of the β-decay transition rates is not possible even when a $K^\pi = \frac{3}{2}^+$ band based on a hole in orbit No. 7 is mixed in with the $K = \frac{3}{2}^+$ orbit No. 8 wave functions for the 1.273- and 3.069-MeV states.

The spectroscopy of the Si^{29} levels is not very well known[9] above the level at 4.08 MeV. These measurements are of some interest. For example, the properties of the $\frac{7}{2}^+$ and $\frac{9}{2}^+$ states belonging to the $K = \frac{1}{2}$ and $\frac{3}{2}$ bands are predicted by the strong-coupling model. It would be interesting to locate

these states and compare their properties with the predictions of this model. Also interesting is the decay of the state at 4.89 MeV, which has been characterized as the "antianalog" state.[10] This report describes a study of the properties of Si^{29} levels with excitation energies between 4.08 and 6.38 MeV.

Mg^{26} targets were bombarded by α particles at several incident energies in the neighborhood of 5–8 MeV; resulting γ radiation was detected in Ge(Li) detectors. Angular-correlation and lifetime measurements were performed. For the angular-correlation measurements, strong alignment, i.e., unequal population of the magnetic substates of the residual nuclei, was produced by choosing α bombarding energies near the threshold energy for production of the state of interest. The γ-ray angular correlations may then be readily analyzed in terms of level spin and multipole mixing.[11] The measurements are described in Sec. II, while Sec. III describes the deduction of level spins and multipole mixtures from the measured correlations. Nuclear lifetimes were deduced using the Doppler-shift-attenuation method (DSAM).[12] This work is described in Sec. IV. A detailed summary of the electromagnetic decay properties of Si^{29} for levels with $E_x < 6.38$ MeV is also presented here. Section V is a discussion section and includes a critique of the method used to obtain level spins and multipole mixtures and a comparison of the properties of Si^{29} with the predictions of both the strong-coupling model and the weak-coupling model. Preliminary descriptions of this work have been given elsewhere.[13]

II. γ-RAY SPECTRUM AND ANGULAR-CORRELATION MEASUREMENTS

Targets of Mg^{26} foil (99.7% Mg^{26})[14] were bombarded by α particles accelerated by the Stanford University tandem Van de Graaff generator. The target foils as obtained from Oak Ridge varied in thickness from 2–10 mg/cm^2 and were used directly in the preliminary experiments. Later, in order to minimize background radiation, these foils were rolled to a thickness ~0.5 mg/cm^2. Bombarding energies were in the energy range of 5–8 MeV. After momentum analysis, the beam was focused by a strong-focusing lens and collimated by a $\frac{1}{16}$-in.-diam circular tantalum aperture, located 1 m from the target. A beam stop of Ta metal was placed directly behind the target. Both target and beam stop were mounted in a cylindrical glass target chamber of 1 in. diameter. Reaction γ radiation was detected with Ge(Li) γ-ray spectrometers.[15] Some early data were recorded with a 20 cm^3 unit, but the majority of data presented here was obtained with a 37-cm^3 right cylindrical diode, 40 mm diam×32 mm long, with an active volume >90%. The response of this latter detector was such that a 5-MeV γ ray produced full-absorption peaks and one- and two-escape peaks of approximately equal height in the pulse-height distribution. The detector was mounted upon a trolley which could be rotated about a vertical axis through the reaction site. Generally, data were collected with the front face of the detector located 15 cm from the reaction site. Also 2.5 cm of paraffin covered the front face of the detector, scattering out some of the reaction neutrons and decreasing neutron-induced radiation damage to the detector. Pulse-height distributions were recorded with a 4096-channel analog-to-digital converter interfaced with a small general-purpose computer.[16,17]

The energy levels of Si^{29} are well known for the excitation energies $E_x < 7$ MeV from charged-particle spectroscopy, while for $E_x < 4.08$ MeV the γ-ray transitions are also well understood.[9] A spectrum taken at $E_\alpha = 6.0$ MeV and $\theta_\gamma = 90°$ was studied thoroughly and the γ rays could all be identified with known transitions in Si^{29} or Mg^{26} [the Mg^{26}-$(\alpha, \alpha')Mg^{26}$ reaction]. The Q value for the Mg^{26}-$(\alpha, n)Si^{29}$ reaction is +0.033 MeV,[9] and by increasing the bombarding energy appropriately, new levels in Si^{29} could be included in the reaction in turn. As the bombarding energy was varied from 6 to 8 MeV in increments of 200 keV, excitation functions were measured at $\theta_\gamma = 55°$ for each new γ ray appearing in the spectrum. Very detailed studies of these singles spectra were made using a computer analysis program for peak location and intensity, including, for the higher-energy γ rays, the excitation functions of the full-absorption, and one- and two-escape peaks.[18] With the aid of these excitation functions we could be sure of correct correspondence between spectral lines and Si^{29} γ-ray transitions. γ radiations from the levels with higher excitation energy were identified by intercomparison with the previous spectra obtained at the lower bombarding energies. Points of comparison included appearance of a new peak in the spectra, its energy, and behavior of the yield curve near threshold. Because of the shape of the neutron s-wave penetrability curve,[19] γ rays produced in the $Mg^{26}(\alpha, n)Si^{29}$ reaction show a pronounced increase near threshold, whereas γ rays produced in the $Mg^{26}(\alpha, p)Al^{29}$ reaction show a much slower increase near threshold. This last reaction was in any case not much of a problem – the Q value is −2.86 MeV, and the reaction was much less prolific than the $Mg^{26}(\alpha, n)Si^{29}$ reaction even at the higher bombarding energies. In this way, γ-ray transitions from all the levels with $E_x \leq 6.38$ MeV

were identified. Two recorded γ-ray pulse-height distributions obtained during extended runs from the excitation function series at $E_\alpha = 6.6$ and 7.4 MeV are illustrated in Fig. 1. The peaks are labeled according to the transitions in Si^{29} to which they are assigned, using the criteria described above. Since transitions which are labeled in Fig. 1(a) are not relabeled in Fig. 1(b), these spectra illustrate nicely the manner in which the γ-ray spectrum changes with energy. We have also illustrated the excitation functions for the γ rays from the 5.28-MeV level in Fig. 2. The change in γ-ray yield with increasing bombarding energy near threshold is illustrated in these curves, as well as the usefulness if not necessity of these excitation functions in sorting out the γ-ray pulse-height distribution. In the figure, the curves labeled (5.28 $\rightarrow$ 2.03), $(5.28 \rightarrow 2.03)_1 + (5.81 \rightarrow 3.07)$, and $(5.28 \rightarrow 2.03)_2 + (5.81 \rightarrow 3.07)_1$ represent the excitation functions for these γ-ray peaks, the latter two degenerate in energy. Because these three curves do not have the same shape, it was clear that the excitation curves for $(5.28 \rightarrow 2.03)_{1,2}$ included a contribution from another γ ray(s), subsequently determined to be a γ ray due to the $5.81 \rightarrow 3.07$ transition both from its energy and the excitation function of the 5.81-MeV state. The curves labeled $(5.28 \rightarrow 2.03)_1$ and $(5.28 \rightarrow 2.03)_2$ are drawn with the shape of the $(5.28 \rightarrow 2.03)$ excitation function, and normalized to the $5.28 \rightarrow 2.03$ yield at 6.6 MeV using the known counter efficiency. The yield curves for the $5.81 \rightarrow 3.07$ transition obtained from subtracting the estimated $(5.28 \rightarrow 2.03)_{1,2}$ γ ray in the experimental curves are consistent with the exci-

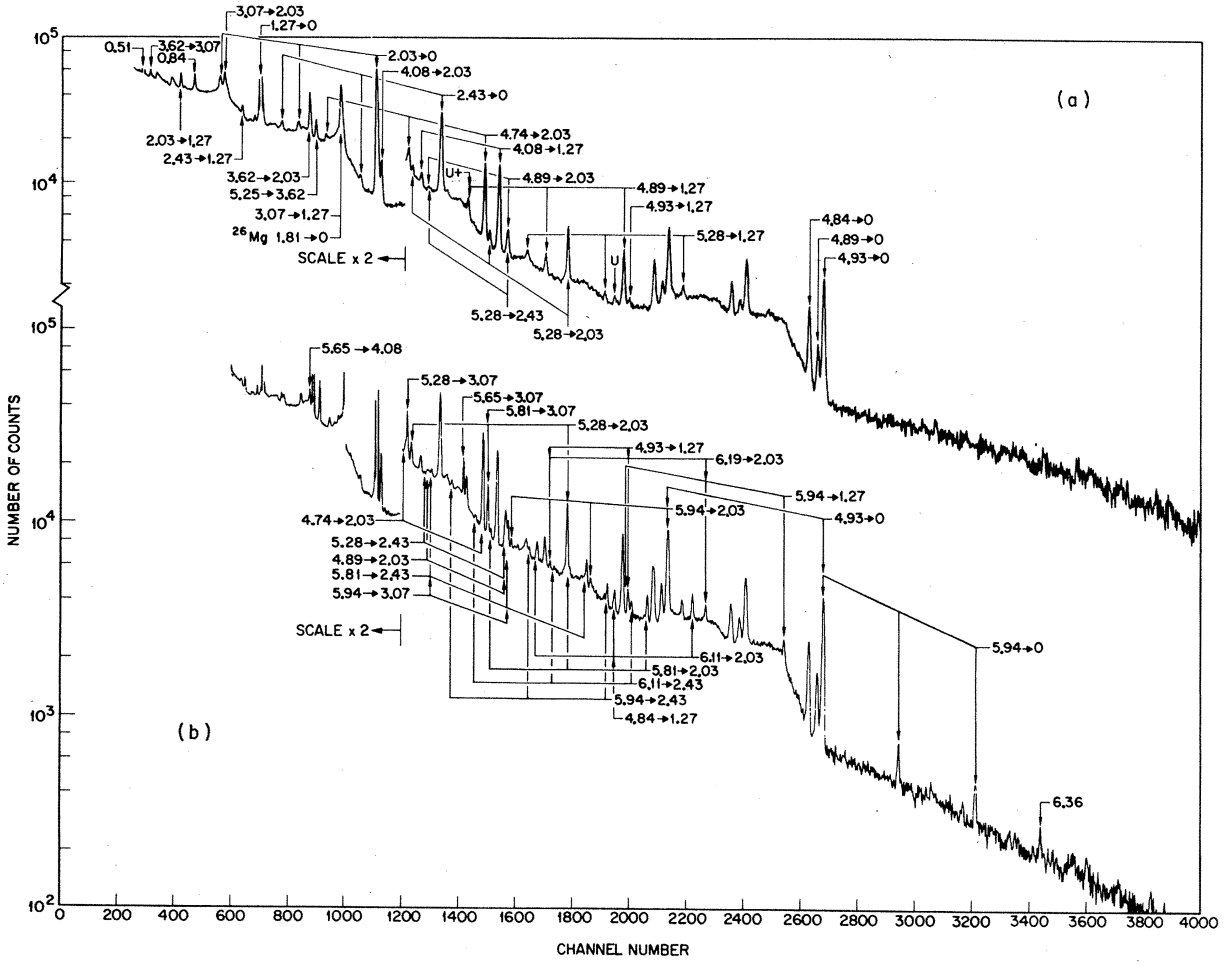

FIG. 1. Pulse-height distributions of γ rays produced in the $Mg^{26}(\alpha, n\gamma)Si^{29}$ reaction at (a) $E_\alpha = 6.6$ MeV and (b) $E_\alpha = 7.4$ MeV. The γ-ray detector was a 37-cm^3 unit, located 15 cm from the target and at $\theta_\gamma = 55°$. Full-energy absorption peaks in the spectrum are labeled by the transition energies (in MeV) in Si^{29} to which they correspond; one- and two-escape peaks are indicated by the lines connecting to the full-energy peaks, except where they are obvious. Spectrum (a) is completely labeled in this fashion while in spectrum (b), except where confusion would result, only transitions not already labeled in (a) are given labels.

tation function of the 5.81-MeV level deduced from the 5.81 → 2.03 transition.

For the more prominent of these reaction-induced γ rays, precision energy measurements were done in two steps. Energies of γ rays >1 MeV were deduced from a γ-ray pulse-height distribution obtained at $\theta_\gamma = 90°$ and $E_\alpha = 6.0$ MeV, in which the activity from a Co^{56} source was recorded simultaneously with the reaction-induced γ rays. Peak centroids were extracted from the pulse-height distribution, and a polynomial of order 2 was fit to the Co^{56} peak locations. Using the energy determinations quoted by Marion,[20] energies of the Si^{29} γ rays with $E_\gamma < 3.5$ MeV were determined by comparison with this calibration line. For $E_\gamma > 3.5$ MeV, the energy separation between two-escape lines and full-energy peaks ($\Delta E = 1.022$ MeV) was used to bootstrap the calibration line. Precision energy determinations were also made for the peaks observed in two other spectra taken at $\theta_\gamma = 90°$ and bombarding energies $E_\alpha = 6.6$ and 7.6 MeV, in order to extend the measurements to γ rays from levels up to an excitation energy of 6.38 MeV in Si^{29}. The energy determinations of the new γ rays in the spectra taken at 6.6 and 7.6 MeV are based on the Si^{29} γ-ray energies obtained at 6.0 MeV, since when the Co^{56} γ rays were included in the spectrum there was so much overlapping of spectral lines that the γ rays due to Co^{56} could not be used as energy standards. For γ rays with energies less than 1 MeV, energy determinations were made from the spectra described above, and also one taken at $E_\alpha = 7.0$ MeV. Calibration was based on three lines in the spectrum, usually the annihilation quantum energy and the Co^{56} γ rays with $E_\gamma = 846.76$ and 1283.34 keV. Table I lists γ-ray energies obtained in this fashion, together with some previous γ-ray energy determinations which are included for comparison. The errors associated with the energy values are due mainly to errors associated with extracting the peak centroids from the spectra. These errors reflect the statistical uncertainty as well as an error associated with the uncertain background line shape. The agreement among the various experimenters seems to be good at lower γ-ray energies, with somewhat less overlap at higher energies, although the number of γ rays for comparison is fewer here. Our energy determination for the 2424.8-keV level is ~1 keV lower than the values of the other experimenters. Precision excitation energies for Si^{29} levels were deduced from these γ-ray energies (after correction for recoil) and are listed in Table II; here level energies deduced from other work are also included to facilitate comparison with our results. Incidentally, the energy of the 3.07-MeV level was determined from the 3.62 → 3.07 transition and the energy of the 3.623-MeV level, since the energies of the cascade γ rays from the 3.067-MeV level were not determined very well. The agreement among the various determinations is good, with the γ-ray work resulting in the most precise values. There are some systematic trends in the energies deduced from the magnetic analysis compared with the results of the γ-ray spectroscopy; above 4-MeV excitation energy the energy determinations of Meyer-Schützmeister *et al.*[10] are apparently too high, while the results of Hinds and Middleton[21] seem to be consistently low. Among the energies deduced from γ-ray work, we see that the energies quoted in Table II generally are in accord within 1 standard deviation except for the 2425- and 4933-keV levels.

The γ-ray yields extracted from the excitation function were corrected for the detector efficiency

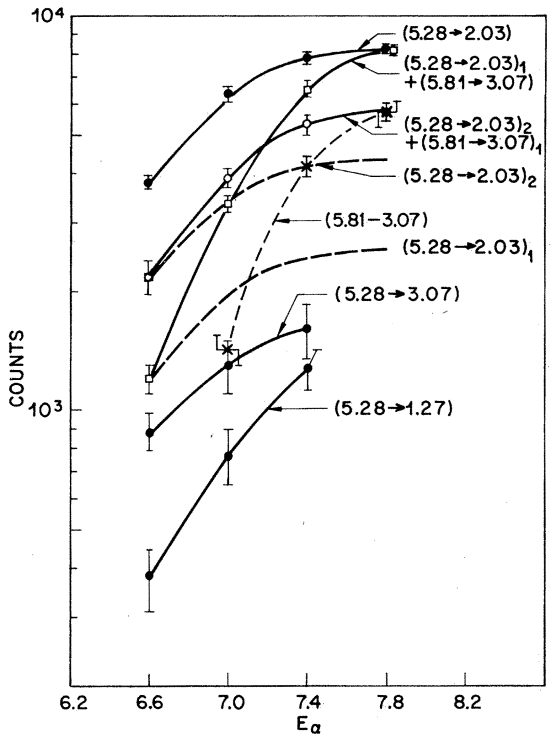

FIG. 2. Excitation functions for the γ-ray transitions of the 5.28- and 5.81-MeV levels labeled by the initial- and final-state energies (MeV). In the Ge(Li) γ-ray spectrum, the one- and two-escape peaks of the 5.28 → 2.03 transition are degenerate in energy with the full-absorption and one-escape peak of the transition 5.81 → 3.07. The excitation functions of the one- and two-escape peaks of the 5.28 → 2.03 transition illustrated by the dashed curve (consistent with the counter efficiency) are drawn with the shape of the excitation function of the 5.28 → 2.03 transition, while the excitation function labeled 5.81 → 3.07 also illustrated with a dashed curve is obtained simply by subtraction.

and then used directly to obtain the level branching ratios. The yields were not corrected for $P_4(\cos\theta)$ terms in the γ-ray angular correlations. Relative γ-ray efficiency curves for the detector were obtained in two steps. For $E_\gamma < 3.5$ MeV, a Co^{56} spectrum was recorded and a relative-efficiency curve was deduced using the intensities of Co^{56} γ rays as given by Marion[20]; for $3.5 < E_\gamma(\text{MeV}) < 8.2$ the shape of the relative efficiency curve was measured using γ-ray yields obtained at two resonances in the $Al^{27}(p,\gamma)Si^{28}$ reaction ($E_p = 1262$[22] and 1724 keV[23]). The two curves were joined with a smooth line, since the shape of the efficiency curve deduced from data obtained in the $Al^{27}(p,\gamma)Si^{28}$ reaction for $E_\gamma < 3.5$ MeV was not well determined. At the 1724-keV resonance, we were not able to continue a smooth extrapolation of the efficiency curve for the full-absorption and one- and two-escape peaks using the γ-ray yields of Anyas-Weiss *et al.*[23] without discounting the peak intensities for $E_\gamma = 5.08$ MeV. We continued the extrapolation of the efficiency curve with the quoted intensities of the higher-energy γ rays. Additional data on the intensity ratio for full-absorption peaks vs one- and two-escape peak intensities were obtained from our data on the transitions near 5 MeV in Si^{29}.

The γ-ray branching ratios obtained in this fashion are listed in Table III. We have also listed branching ratios deduced from other experiments in Table III to facilitate a comparison of results. In these other works branching ratios and errors

TABLE I. Precision γ-ray energies (in keV) obtained in the decay of Si^{29}*.

Transition (E_x in Si^{29}) (keV)	E_γ [$Mg^{26}(\alpha, n\gamma)Si^{29}$][a] $E_\alpha = 6.0$	$= 6.6$	$= 7.0$	$= 7.6$	$\overline{E}_\gamma$ $Mg^{26}(\alpha n\gamma)Si^{29}$ [a]	E_γ $Al^{29}(\beta^-)Si^{29}$ [b]	$E_\gamma(n,\gamma)$ Ref. 25	Ref. 26
2425 → 2028						397.8 ± 0.3		
3623 → 3067	556.4 ± 0.4	555.1 ± 0.5	556.5 ± 0.4	557.0 ± 1.0	556.2 ± 0.2			
4741 → 4080		659.3 ± 1.0		661.1 ± 1.0	660.2 ± 2.2			
2028 → 1273	755.3 ± 0.4	755.8 ± 0.5	756.1 ± 1.5	754.7 ± 1.0	755.5 ± 0.6			
3067 → 2028		1035.3 ± 1.5			1035.3 ± 1.5			
2425 → 1273	1152.1 ± 0.2				1152.1 ± 0.2			1152.6 ± 0.2
1273 → 0	1273.1 ± 0.2				1273.1 ± 0.2	1273.3 ± 0.2	1273.0 ± 0.5	1273.4 ± 0.2
5652 → 4080				1572.2 ± 0.6	1572.2 ± 0.6			
3623 → 2028	1595.5 ± 0.2				1595.5 ± 0.2			
5254 → 3623		1631.0 ± 0.3			1631.0 ± 0.3			1793.5 ± 0.2
2028 → 0	2027.5 ± 0.2				2027.5 ± 0.2	2028.2 ± 0.8 [c]	2031.5 ± 1.0	2028.1 ± 0.5
4080 → 2028		2051.9 ± 0.5			2051.9 ± 0.5			
2425 → 0	2424.8 ± 0.2				2424.8 ± 0.2	2426.2 ± 0.8 [c]	2426.9 ± 1.0	2425.9 ± 0.4
5652 → 3067				2585.3 ± 2.0	2585.3 ± 2.0			
4741 → 2028		2712.8 ± 0.3			2712.8 ± 0.3			
5811 → 3067				2745.3 ± 1.1	2745.3 ± 1.1			
4080 → 1273		2806.3 ± 0.3			2806.3 ± 0.3			
4895 → 2028	2867.0 ± 0.7				2867.0 ± 0.7			
5284 → 2028		3256.3 ± 0.5			3256.3 ± 0.5			
4895 → 1273	3621.6 ± 0.4				3621.6 ± 0.4			
4933 → 1273							3661.5 ± 2.0	3660.9 ± 0.4
6107 → 2425				3680.0 ± 1.0	3680.0 ± 1.0			
5811 → 2028				3782.8 ± 0.8	3782.8 ± 0.8			
6381 → 2425							3954.2 ± 1.0	3954.4 ± 0.5
6107 → 2028				4078.8 ± 0.5	4078.8 ± 0.5			
6191 → 2028				4161.9 ± 1.2	4161.9 ± 1.2			
4838 → 0	4837.7 ± 0.8				4837.7 ± 0.8			
4895 → 0	4893.8 ± 1.2				4893.8 ± 1.2			4839.7 ± 0.5
4932 → 0	4931.9 ± 0.6				4931.9 ± 0.6		4933.4 ± 1.0	
6381 → 1273							5107.8 ± 1.0	5106.6 ± 0.6
5946 → 0				5945.6 ± 3.0	5945.6 ± 3.0			
6381 → 0				6376.0 ± 3.0	6376.0 ± 3.0		6380.1 ± 1.0	6379.8 ± 3.0

[a] This experiment; $\theta_\gamma = 90°$.
[b] W. R. Harris, K. Nagatani, and D. Alburger, Phys. Rev. 187, 1445 (1969).
[c] Reference 8.

are not quoted directly, and we have deduced the numbers of Table III from the quoted relative γ-ray intensities. Our branching-ratio measurements for the 6.38-MeV level are poor, e.g., we did not observe the 6.38 → 2.43 transition. This is because the level was not strongly excited at E_α = 7.8 MeV, where the branching ratios were deduced. Generally speaking, the agreement with the work of Spits, op den Kamp, and Grumppelaar[24] and Lycklama, Hughes, and Kennett[25] is good, while we do not observe several of the transitions reported by Dickens.[26] The branching of the 4.84 → 1.27 transition is given by Dickens[26] as (35 ± 9)%, whereas we quote (10 ± 1)%. Above E_α = 7 MeV, spectral peaks due to this transition become confused with the escape peaks of the 6.11 → 2.03 transition, which may account for this discrepancy. Our value of 10% is obtained from the data collected at E_α = 7.0 MeV, where the 4.84-MeV level has maximum excitation. We have studied our spectra in detail to search for several strong transitions listed by Dickens which we did not observe, namely the 5.25 → 3.07, 4.89 → 2.43, and 4.74 → 3.63 transitions (see Table III). The 5.25 → 3.07 and 4.74 → 3.63 transitions did not appear in our spectrum. We used background statistics in spectra measured at E_α = 6.6 and 7.0 MeV at the energy of these γ rays to estimate upper limits (2 standard deviations) for these transitions of 3 and 1%, respectively. The 4.89 → 2.43 transition might possibly be evident in the spectrum at E_α = 6.2 MeV, where if present, it is mixed in with the Compton edge of the 4.74 → 2.03 transition. We estimate a yield for the 4.89 → 2.43 transition and obtain a limit (2 standard deviations) for the branching of 5%.

Once all the lines in the γ-ray spectra were assigned, angular correlations were deduced from pulse-height distributions recorded with the counter at angles (in degrees) θ_γ = 0, 30, 45, 60, and 90 with respect to the incident beam direction for a fixed amount of charge, usually 3000 μC. We generally repeated the 0, 45, and 90° measurements. The γ-ray yields at the various θ_γ were normalized to both integrated charge and to the yield of the isotropic 4.84 → 0 transition. Both normalizations produced angular correlations consistent within experimental error. Beam currents were about 60–80 nA, and a typical run required about 2 h. The integral counting rate was about $3-4\times10^3$ counts/sec. Yields of the various γ rays were obtained by fitting a polynomial to the background underneath the spectrum peak corresponding to the γ ray of interest and extracting the peak area for each θ_γ. Errors associated with the measured yields were compounded of the statistical

TABLE II. Energy levels (in keV) of Si^{29} from $Mg^{26}(\alpha, n\gamma)Si^{29}$, $Si^{28}(n, \gamma)Si^{29}$, $Al^{27}(He^3, p)Si^{29}$, $Si^{28}(d, p)Si^{29}$, $Si^{29}(p, p')Si^{29}$, and $Al^{29}(\beta^-)Si^{29}$.

				He^3, p		d, p		
α, n	n, γ		β^-		Ref. b	Ref. b		p, p'
This experiment	Ref. 25	Ref. 24	Ref. a	Ref. 10	all ± 10	all ± 10	Ref. c	Ref. d
1273.1 ± 0.2	1273.0 ± 0.5	1273.3 ± 0.2	1273.3 ± 0.2	1271		1270	1278 ± 7	1278 ± 6
2027.6 ± 0.2	2031.5 ± 1.0	2028.0 ± 0.6	2027.8 ± 0.4	2026		2028	2027 ± 7	2027 ± 6
2425.0 ± 0.4	2426.9 ± 1.0	2425.9 ± 0.3	2425.7 ± 0.4	2425		2426	2426 ± 7	2924 ± 6
3066.9 ± 0.5		3067.0 ± 0.4		3070		3067	3070 ± 7	3064 ± 6
3623.1 ± 0.3				3623		3621	3623 ± 7	3620 ± 6
4079.5 ± 0.4				4085		4074	4078 ± 8	4079 ± 6
4740.5 ± 0.4				4753	4736	4735		4735 ± 6
4838.5 ± 0.8		4840.3 ± 0.4		4843	4837	4833	4840 ± 8	4833 ± 6
4894.9 ± 0.6				4903	4887	4890	4897 ± 8	4891 ± 6
4932.6 ± 0.4	4933.4 ± 1.0	4934.3 ± 0.4		4935	4920	4924	4934 ± 8	4930 ± 6
5254.1 ± 0.5				5260	5250	5251		5244 ± 7
5284.4 ± 0.7				5291	5280	5280		5274 ± 7
5651.8 ± 0.7				5660	5646	5644		5646 ± 7
5810.7 ± 1.2				5822	5808	5806		5804 ± 7
5946.3 ± 3.0				5962	5945	5942	5946 ± 9	5937 ± 7
6106.6 ± 0.6				6120	6102	6101	6105 ± 9	6098 ± 7
6190.7 ± 1.3				6206	6184	6186		6189 ± 7
6378.8 ± 3.0	6380.1 ± 1.0	6380.5 ± 0.5		6387	6371	6370	6380 ± 9	6380 ± 7

[a] W. R. Harris, K. Nagatani, and D. E. Alburger, Phys. Rev. 187, 1445 (1969).
[b] S. Hinds and R. Middleton, private communication, quoted in R. E. White, Phys. Rev. 119, 767 (1960).
[c] D. M. Van Patter and W. W. Buechner, Phys. Rev. 87, 51 (1952).
[d] White, Ref. b.

uncertainty of the peak area and of an estimate of the uncertainty associated with the background line shape. Attenuation coefficients for this counter, located with its front face 15 cm from the target, are $Q_0 = 1.00$, $Q_2 = 0.99$, and $Q_4 = 0.97$.[27] A summary of the angular correlations measured in this study, sequenced according to level energy, γ-ray transition energy, and α-particle bombarding energy, is presented in Table IV. The tabulated coefficients represent a least-squares fit to the expansion

$$W(\theta) = 1 + A_2 P_2(\cos\theta) + A_4 P_4(\cos\theta) . \quad (1)$$

We also list the quantity

$$\chi^2 = \frac{n}{n-2} \sum_1^n \frac{[W_i(\theta) - Y_i(\theta)]^2}{\Delta Y_i(\theta)^2} . \quad (2)$$

Here n denotes the number of data points, and $Y_i(\theta)$, $\Delta Y_i(\theta)$ denote the measured yield and its associated error measured at θ_γ. We note that all the angular correlations except those of the 4.84 $\rightarrow$ 0 and 6.38 $\rightarrow$ 0 transition require an A_2 coefficient in the Legendre polynomial expansion, and thus these levels all have $J \geq \frac{3}{2}$. Some typical correlations will be illustrated in the next section, where the analysis is discussed.

All possible angular correlations which could be extracted from the collected data are not listed in Table III, only those to be treated in subsequent analysis as angular correlations from aligned nuclei according to the description of Litherland and Ferguson.[28] This analysis and its justification are considered in the next section.

III. ANALYSIS OF THE ANGULAR CORRELATIONS IN TERMS OF LEVEL SPIN AND MULTIPOLE MIXTURES

Litherland and Ferguson have described two general methods for the deduction of nuclear level spin and determination of multipole mixtures in γ-ray transitions from measurements of the γ-ray angular correlation following the decay of aligned nuclei produced in nuclear reactions.[28] The first procedure (Method I) involves measurements of γ-

TABLE III. Branching ratios (%) of electromagnetic decay modes of excited states in Si^{29} with $4.74 \leq E_x(\text{MeV}) \leq 6.38$.

State (MeV)		Decay to 0.0	1.27	2.03	2.43	3.07	3.62	4.08	4.84	4.93
4.74	a			94 ± 1			<1 [g]	6 ± 1		
	b			69 ± 17			31 ± 17			
4.84	a	90 ± 1	10 ± 1							
	b	65 ± 9	35 ± 9							
4.90	a	20 ± 1	56 ± 3	24 ± 1	<5					
	b	25 ± 3	62 ± 3		13 ± 4					
	c	20	50	30						
4.93	a	95 ± 1	5 ± 1	<1	<1	<2				
	b	81 ± 8	19 ± 8							
	d	94 ± 1	5 ± 1	0.1 ± 0.05	0.2 ± 0.1	0.8 ± 0.2				
	e	94 ± 1	6 ± 1							
5.25	a					<3	100 [h]			
	b					≥67				
5.28	a		11 ± 1	67 ± 2 [f]	13 ± 1	9 ± 1				
5.65	a					44 ± 11		56 ± 11		
5.81	a			22 ± 3	27 ± 5	51 ± 10				
5.95	a	14 ± 2	23 ± 4	15 ± 3	22 ± 4	26 ± 3				
6.11	a			66 ± 3	34 ± 3					
6.19	a			100						
6.38	a	76 ± 3	24 ± 3		<9					
	d	63 ± 1	20 ± 2		11 ± 1				<10	<10
	e	70 ± 1	22 ± 2		8 ± 1				2 ± 1	4 ± 2

[a] This experiment.
[b] Reference 26.
[c] Reference 10.
[d] Reference 24.
[e] Reference 25.
[f] This transition also reported in Ref. 10.
[g] Limits are 2 standard deviations.
[h] In general, unobserved branches are estimated as ≤10% except where other limits are quoted.

γ angular correlations following the decay of the residual nucleus, from which the unknown population parameters of the γ-ray emitting level, together with the nuclear spins and γ-ray transition multipolarity may be determined. The second procedure (Method II) requires the use of a particle counter located along the beam axis, either at 0 or 180° relative to the incident beam direction, and measurement of p-γ angular correlations. The quantum numbers of the magnetic substates of the residual nuclei, m, are restricted to the sum of the nuclear spins of the target, incident particle, and outgoing light particle. In the first procedure the population parameters are determined, while the second procedure depends on restricting the population parameters. Both methods have been heavily exploited in reaction-independent measurements of nuclear level spins. Another technique

TABLE IV. Description of the γ-ray angular correlations in terms of the Legendre polynomial expansion, $W(\theta) = 1 + A_2 P_2(\cos\theta) + A_4 P_4(\cos\theta)$.

E_x (MeV)	E_γ (MeV)	Transition	E_α (MeV)	A_2	A_4	χ^2
4.08	2.81	4.08→1.27	5.2	0.47±0.02	−0.36±0.03	1.1
		4.08→2.03	5.2	−0.04±0.05	−0.03±0.05	2.2
4.74	2.71	4.74→2.03	5.8	0.33±0.03	−0.22±0.03	1.6
			6.0	0.38±0.01	−0.25±0.02	1.9
			6.2	0.42±0.01	−0.25±0.02	0.2
4.84	4.84	4.84→0	6.2	−0.01±0.04	0.04±0.04	0.6
			6.4	0.06±0.05	−0.07±0.05	0.9
4.90	2.87	4.90→2.03	6.0	0.33±0.11	0.14±0.12	1.2
			6.2	0.31±0.04	0.10±0.04	0.3
			6.4	0.32±0.04	−0.03±0.04	2.4
	3.62	4.90→1.27	6.0	−0.25±0.03	−0.07±0.03	0.5
			6.2	−0.27±0.02	0.03±0.02	3.3
			6.4	−0.23±0.03	0.05±0.03	1.4
	4.90	4.90→0(2)	6.0	0.42±0.06	−0.33±0.07	0.7
		4.90→0	6.2	0.52±0.03	−0.31±0.04	0.6
		4.90→0(2)	6.2	0.47±0.04	−0.36±0.04	1.9
4.93	4.93	4.93→0	6.0	−0.37±0.03	0.02±0.03	1.0
			6.2	−0.43±0.02	0.01±0.02	0.3
			6.4	−0.34±0.02	0.01±0.02	3.9
5.25	1.63	5.25→3.62	6.2	0.39±0.09	0.03±0.10	0.6
			6.4	0.55±0.03	0.13±0.03	1.6
			6.6	0.47±0.03	0.08±0.03	1.5
5.28	3.26	5.28→2.03	6.4	−0.66±0.02	−0.01±0.02	1.2
			6.6	−0.56±0.03	−0.03±0.02	2.1
	4.01	5.28→1.27	7.2	0.53±0.06	−0.33±0.07	1.1
			7.4	0.59±0.08	−0.19±0.09	0.5
5.65	1.57	5.65→4.08	7.2	0.33±0.04	−0.13±0.04	2.3
			7.4	0.30±0.06	−0.23±0.06	1.1
			7.6	0.16±0.06	−0.07±0.07	0.9
	2.59	5.65→3.07	7.2	0.33±0.04	−0.14±0.03	0.5
			7.4	0.36±0.05	−0.27±0.05	0.7
5.81	3.79	5.81→2.03	7.2	−0.72±0.06	0.30±0.06	1.8
			7.4	−0.69±0.08	0.37±0.08	2.8
			7.6	−0.65±0.06	0.34±0.05	0.9
5.95	5.95	5.95→0(1)	7.4	−0.47±0.08	0.12±0.08	1.0
6.11	4.08	6.11→2.03	7.6	0.39±0.03	0.01±0.03	0.8
	3.68	6.11→2.43	7.6	−0.28±0.07	−0.03±0.06	0.2
6.19	4.16	6.19→2.03	7.6	−0.22±0.05	−0.05±0.05	0.2
			7.8	−0.27±0.03	−0.08±0.03	1.3
6.38	6.38	6.38→0	7.8	−0.15±0.07	−0.07±0.08	0.4

of producing strong alignment of recoiling nuclei following a nuclear reaction is by initiating the reaction near the threshold energy; the l value of the outgoing partial waves will usually be predominantly $l=0$ and the residual nucleus will be left in magnetic substates with low magnetic quantum numbers.[11] In the present case, the $Mg^{26}(\alpha, n)Si^{29}$ reaction initiated at α bombarding energies 200–600 keV above threshold, a rough estimate of the alignment of the residual nuclei may be made from calculated s- and p-wave neutron penetrabilities T_l with the assumption that the outgoing neutron transmission coefficient T_l (weighted by $2l+1$) dominates the reaction cross section.[19] For example, for $E_n=300$ keV, $T_s/T_p=7.8$. If channel spins $\frac{1}{2}$ and $\frac{3}{2}$ are equally probable, 75% of the p-wave neutrons will have $(l+s)_z=\frac{1}{2}$ and 25% will have $(l+s)_z=\frac{3}{2}$. Hence, approximately 93% of the outgoing neutrons leave the residual nucleus with $|m|=\frac{1}{2}$, the same restriction which results from the collinear geometry (Method II). More sophisticated estimates of transmission coefficients may be made with the optical model,[29] while if one assumes a particular reaction model the $P(m)$'s may be calculated directly.

In view of the above, analysis of the angular correlations listed in Table IV in terms of the population parameters, level spins, and γ-ray multipole mixing ratios can be done using the Method II formulas given by Litherland and Ferguson.[28] A description of the procedure we use has been given by Poletti and Warburton.[30] In fitting the experi-

TABLE V. Some results of direct-reaction studies of Si^{29} using the reactions $Si^{28}(d,p)Si^{29}$, $Al^{27}(He^3,p)Si^{29}$, $Si^{30}(He^3,\alpha)Si^{29}$, and $Si^{30}(d,t)Si^{29}$.

E_x	(He^3,p) [a]		(d,p) [b,c]				(He^3,α); (d,t) [d]	
(MeV)	L_{tot}	J^π	l_n	J^π	$(2J+1)\theta_n^2$	θ_{Rel}^2	J^π	S
0	2		0	$\frac{1}{2}^+$	46	1		0.8
1.27	0, 2		2	$(\frac{3}{2}, \frac{5}{2})^+$	70	1.5		0.9
2.03	0		2	$(\frac{3}{2}, \frac{5}{2})^+$	28	0.4		1.7
2.43	0		2	$(\frac{3}{2}, \frac{5}{2})^+$	<1.2			0.19
3.07	0, 2		2	$(\frac{3}{2}, \frac{5}{2})^+$	16	0.2		0.14
3.62	Odd		3	$(\frac{5}{2}, \frac{7}{2})^-$	130	2.2		0.09
4.08	(0, 2)	(+)	Isotr.					
4.74	2	$(\frac{1}{2}^+)$						
4.84			0	$\frac{1}{2}^+$				
4.90	0		Isotr.				$(\frac{5}{2})^+$	1.0
4.93	Odd	(−)	1	$(\frac{1}{2}, \frac{3}{2})^-$	120			
5.25			Isotr.					
5.28	0	(+)	Isotr.					
5.65	2	$(\frac{1}{2}^+)$						
5.81	0	(+)						
5.95	0	(+)	2	$(\frac{3}{2}, \frac{5}{2})^+$	(8)			
6.11	Odd	(−)	Weak		(13)			
6.19	Odd	(−)	3	$(\frac{5}{2}, \frac{7}{2})^-$	43			
6.38	Odd	(−)	1	$(\frac{1}{2}, \frac{3}{2})^-$	65			
6.72	0, 2	(+)					$(\frac{5}{2})^+$	0.3
8.31	0						$(\frac{5}{2})^+$	1.8

[a] Reference 10.
[b] Reference 33.
[c] Reference 9.
[d] Reference 37. For the (d,t) and (He^3,α) reactions S is the average value; the $J^\pi=\frac{5}{2}^+$ assignments are due to J-dependence effects.

mental angular correlations to the theoretical formulas, the magnetic quantum numbers of residual nuclear states were restricted to $|m| \leq \frac{3}{2}$. Where possible, level spins and multipole mixtures were obtained with $P(\frac{1}{2})$ and $P(\frac{3}{2})$ treated as free parameters; otherwise an upper limit $P(\frac{1}{2})/P(\frac{3}{2}) > 0.50$ was imposed to restrict the alternative spin assignments. The analysis is presented in the form of plots of χ^2 vs γ-ray multipole mixing. When the population parameters are not well determined, it is difficult to deduce accurate multipole mixing ratios from these data, since the uncertainty in the magnetic substate populations may broaden the minimum in the χ^2 curve or give more than one minimum. Established spins of the low-lying levels needed in the analysis were taken as $J(0) = \frac{1}{2}$, $J(1.28) = \frac{3}{2}$, $J(2.03) = \frac{5}{2}$, $J(2.43) = \frac{3}{2}$, $J(3.07) = \frac{5}{2}$, and $J(3.62) = \frac{7}{2}$.[9] In one case, we needed $J(4.08)$, which was taken to be $J = \frac{7}{2}$.[31]

Frequently the angular correlation of one particular γ-ray transition was recorded at several energies; these data could be analyzed together, allowing the population parameters to vary at each energy but with the γ-ray multipole mixture fixed. Thus, one improves the statistics and requires a mutual consistency among these data. This technique proved to be of some limited use in rejecting some spin values and mixing ratios.

Another feature of the analysis was that we could not analyze the γ-ray members of cascade transitions simultaneously, e.g., the two γ rays in the 4.90 → 1.27 → 0-MeV cascade, as is frequently the case when a particle detector with energy discrimination is employed in the standard Method II treatment. This was not a severe disadvantage, since frequently the information gained from including the second members of the γ-ray cascade in the analysis is not sufficient to restrict the spin assignment to a unique value.

Levels in the region of excitation energy explored here which have been given unique spin and parity assignments are $J^\pi(4.08) = \frac{7}{2}^+$,[31,32] $J^\pi(4.74) = \frac{9}{2}^+$,[32] $J^\pi(4.84) = \frac{1}{2}^+$,[33] $J^\pi(4.93) = \frac{3}{2}^-$,[34-36] and $J^\pi(6.38) = \frac{1}{2}^-$[34-36]; however, several more levels have alternative spin and parity values which have been deduced from direct-reaction investigations. Since we shall refer to them often, the results of the direct-reaction investigations are summarized in Table V. In this table, we have listed the 4.90-MeV level as $J^\pi = (\frac{5}{2})^+$; Dehnhard and Yntema have invoked J-dependence effects in the differential cross sections and assigned the $J = \frac{5}{2}$ alternative to this level.[37] The same effect, however, results in a $J = \frac{3}{2}$ assignment for the 3.07-MeV level which is known to have $J = \frac{5}{2}$[31]; we have therefore preferred caution and listed these states as $J^\pi = (\frac{5}{2})^+$ in Table V. The spin and parity assignments in column 3 arising from the (He^3, p) work are all described as tentative and thus are enclosed in parentheses.[10]

In the remainder of this section the experimental information resulting from this and previous work will be compared and synthesized to arrive at level spin assignments for Si^{29}. We begin with those levels which received definite spin assignments in this work: $J(4.90) = \frac{5}{2}$, $J(4.93) = \frac{3}{2}$, $J(5.25) = \frac{9}{2}$, $J(5.81) = \frac{7}{2}$, $J(5.95) = \frac{3}{2}$. The analysis used to arrive at the spin assignment and γ-ray multipole mixing for the 4.90-MeV level illustrates the procedure well. The angular correlations measured at $E_\alpha = 6.2$ MeV for the 4.90 → 0, 4.90 → 1.27, and 4.90 → 2.03 transitions are illustrated in Fig. 3. The Legendre expansion coefficients of these correlations are listed in Table IV. Because the 4.90 → 0 transition requires a $P_4(\cos\theta)$ coefficient, we have $J(4.90) \geq \frac{5}{2}$; on the other hand, an argument based on the measured mean life for this level ($\tau = 0.10 \pm 0.03 \times 10^{-13}$ sec) together with the Weisskopf estimates[8] restricts $J(4.90)$ to $\leq \frac{7}{2}$. When the measured angular correlations (3 each) for the 4.90 → 0 and 4.90 → 1.27 transitions were fit in turn

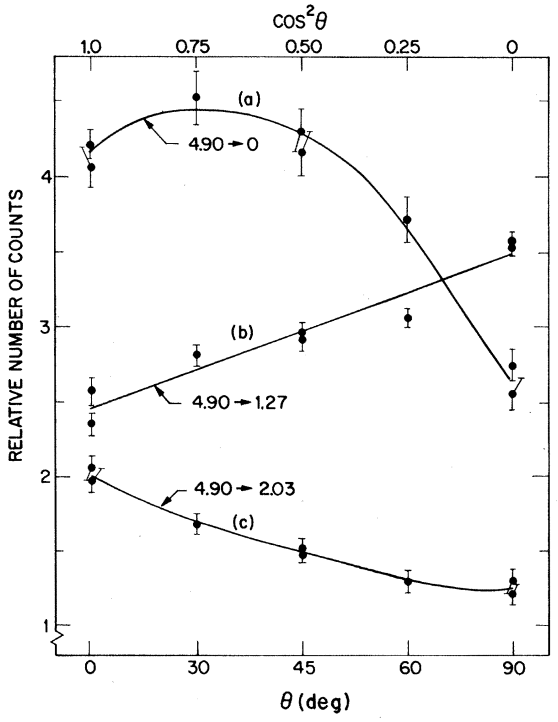

FIG. 3. Three angular correlations measured for γ-ray transitions from the 4.90-MeV level: the 4.90 → 0 (a), 4.90 → 1.27 (b), and 4.90 → 2.03 (c) transitions. The level was populated in the $Mg^{26}(\alpha, n)Si^{29}$ reaction, at $E_\alpha = 6.2$ MeV. The γ-ray detector was a Ge(Li) solid-state detector with nominal volume of 37 cm^3, located 15 cm from the reaction site. The yields represent the area of the full-energy absorption peak after background subtraction.

to the correlation formula, the 4.90 → 0 correlation allowed both alternatives for $J(4.90)$, but the 4.90 → 1.27 correlation restricted the 4.90-MeV level spin to $J=\frac{5}{2}$. This assignment agrees with the preferred assignment $J^\pi=(\frac{5}{2})^+$ for the 4.90-MeV level, which invoked the J-dependence effect.[37] In the fit to the 4.90 → 1.27 transition, $\delta(4.90\rightarrow 1.27)$ was not well defined, but restricted to the interval $-5^\circ \leq \tan^{-1}\delta \leq 10^\circ$, or $-(74.5\pm 1.5)^\circ$. In order to deduce this multipole mixing, it was necessary to use the $P(m)$'s determined from the fit to the angular correlation of the 4.90 → 0 transition. This fit is illustrated in Fig. 4. We see that for $J=\frac{5}{2}$, four alternative values of $\delta(4.90\rightarrow 0)$ were permitted, with values (in deg) of $\tan^{-1}\delta = -79\pm 2.5$, -30 ± 2.0, 1 ± 1.5, and 70 ± 2. Since the state has $\pi=+1$,[37] of the four alternatives for $\delta(4.90\rightarrow 0)$, only $\tan^{-1}\delta=(1\pm 1.5)^\circ$ is consistent with systematics of octupole-quadrupole multipole mixing. The first two solutions may also be rejected as inconsistent with our *ad hoc* upper limit of $P(\frac{3}{2})=50\%$, since they both represent a solution of the angular-correlation equation with $P(\frac{3}{2})=70\%$. (It is perhaps of interest to note these other solutions require $M3$ strengths $|M|^2\approx 10^5$, an enhancement which we may safely reject.) Next, the angular correlations of these two transitions were fit simultaneously to the correlation formula, with $\delta(4.90\rightarrow 0)$ restricted to $\tan^{-1}\delta=(1\pm 1.5)^\circ$, in order to obtain $\delta(4.90\rightarrow 1.27)$. This procedure results in $\tan^{-1}\delta(4.90\rightarrow 1.27)=-(2\pm 1)^\circ$. Similarly, a simultaneous fitting of the angular correlations of the 4.90 → 0 and 4.90 → 2.03 transitions to the correlation formulas results in $\tan^{-1}\delta(4.90\rightarrow 2.03)=(2\pm 3)^\circ$. Errors quoted above and throughout this section for multipole mixtures are statistical only, representing 1 standard deviation and do not include an estimate of the systematic error; this will be introduced later when the multipole mixtures are summarized.

For the 4.93-, the 5.25-, and the 5.81-MeV levels, deduction of the spin assignments from the angular correlations was much more straightforward. Analysis of the 4.93 → 0-MeV correlation limits $J(4.93)$ to $\frac{3}{2}$, and gives $\delta(4.93\rightarrow 0)$ to within wide limits which include $\delta=0$; this is consistent with previous work[34,35] which assigns $J^\pi(4.93)=\frac{3}{2}^-$, $\delta(4.93\rightarrow 0)=0$. The analysis of the angular correlation of the 5.25 → 3.62 transition which results in a $J^\pi=\frac{9}{2}^{(-)}$ assignment and multipole mixing $\delta(5.25\rightarrow 3.62)=-0.49$ has been discussed in detail elsewhere[13] and will not be reproduced here. This is a new assignment. We remark in passing that this assignment and the multipole-mixing value depend on definite assumptions for the population parameters, $P(\frac{1}{2})$ and $P(\frac{3}{2})$. Spear *et al.*[38] have deduced $\pi=-1$ for the 5.25-MeV level from a recent measurement of the 5.25 → 3.62-MeV γ ray. The 5.81-MeV level is previously unassigned. The combined χ^2 curves resulting from fits to the angular correlations of the 5.81 → 2.03 transition measured at $E_\alpha=7.2$, 7.4, and 7.6 MeV are illustrated in Fig. 5. This is a clear-cut case. It is clear from the figure that the only allowed assignment for the 5.81-MeV level is $J=\frac{7}{2}$, and that $\tan^{-1}\delta(5.81\rightarrow 2.03)=+(65.5\pm 1.2)^\circ$. This mixing ratio suggests $\pi=+1$ for the 5.81-MeV level. To see this, first assume $\pi=-1$; then the 5.81 → 2.03 transition has multipolarity $E1$-$M2$. If we combine the limit for the width of this level, $\Gamma_\gamma>33$ meV, the branching ratio 22%, and the mixing ratio $\tan^{-1}\delta=65.5^\circ$, we find $|M(M2)|^2>55$ Weisskopf units (W.u.).[39] On the other hand, the assumption $\pi=+1$ results in $|M(E2)|^2>1.7$ W.u. We suggest $\pi=(+1)$ for this level. This is in accord with parity $\pi=(+1)$ for this level, suggested by Meyer-Schützmeister *et al.*[10]

A unique spin assignment $J=\frac{3}{2}$ is deduced for the 5.95-MeV level from analysis of the 5.95 → 0 correlation. We are not able to deduce the multipole mixing for this level, except within rather wide limits, without invoking a value for $P(\frac{3}{2})/P(\frac{1}{2})$. The level is populated via an $l_n=2$ transition in the Si^{28}-$(d,p)Si^{29}$ reaction[35]; hence $J^\pi=\frac{3}{2}^+$.

Restrictions on all the spin assignments of the remaining levels in this region of excitation energy were obtained and are discussed next. For the 4.08-MeV level, analysis of the angular-correla-

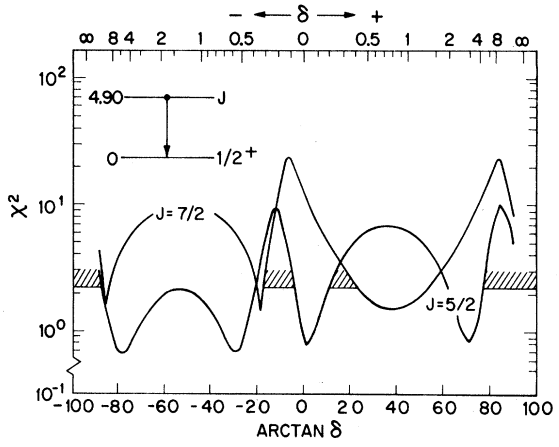

FIG. 4. Curves of χ^2 vs arctanδ(4.90) which result when all the measured angular correlations of the 4.90 → 0-MeV transition are fit to the correlation formulas. The three correlations included are those of the two-escape peak measured at $E_\alpha=6.0$ and 6.2 MeV, and of the full-absorption peak measured at 6.2 MeV. The curves are labeled by assumed values of level spin for the 4.90-MeV state; the spin of the ground state was taken to be $\frac{1}{2}$. The cross-hatched line is the usual 0.1% χ^2 confidence limit.

tion data for the 4.08 → 1.27 transition gives alternative assignments $J=\frac{5}{2}$, $\frac{7}{2}$, or $\frac{9}{2}$. The $J=\frac{9}{2}$ alternative may be ruled out on the basis of the lifetime measurements and electromagnetic transition rate sum rules,[38] and in any case is inconsistent with earlier work.[7] The *ad hoc* upper limit for $P(\frac{3}{2})$ of 50% mentioned above eliminates the $J=\frac{5}{2}$ alternative and we are left with $J(4.08)=\frac{7}{2}$. This spin assignment agrees with other results. Ferguson *et al.*[31] have given a $\frac{7}{2}$ assignment to this level deduced from the γ-γ angular correlation of the 4.08 → 1.27 → 0 cascade. Pilt *et al.*[32] also deduce $J=\frac{7}{2}$ (as well as $\pi=+1$) from a measurement of the γ-ray angular correlation and linear polarization of the 4.08 → 1.27 transition. Nightingale, McDonald, and Becker[40] have also investigated the 4.08-MeV level by measuring the angular correlations of the four decay γ rays from the 4.08-MeV level, i.e., the 4.08 → 1.27 → 0 and the 4.08 → 2.03 → 0 cascade γ rays, in a collinear geometry. The Si^{28}-$(d,p)Si^{29}$ reaction was used to populate the 4.08-MeV level, and γ-p coincident pulse-height distributions were measured. The charged particles were detected in an annular counter located at 180°. Analysis of the correlation of the 4.08 → 1.27 transition results in a $J=\frac{7}{2}$ assignment for the 4.08-MeV level, with the $J=\frac{5}{2}$ alternative rejected at the 1% confidence level. For the mixing ratio of the 4.08 → 1.27 transition, we find that $\delta(4.08\rightarrow 1.27)=+0.03\pm 0.03$. This is consistent with the expected pure $E2$ nature of this transition. We also extracted the correlation of the 4.08 → 2.03 transition, and made a simultaneous fit of this correlation together with that of the 4.08 → 1.27 transition for $J(4.08)=\frac{7}{2}$ and $\delta(4.08\rightarrow 1.27)=0.03$. We find $\delta(4.08\rightarrow 2.03)=-0.14\pm 0.03$. Agreement with other values reported of this multipole mixing is good. Ferguson *et al.*[31] give $\delta=-0.05$ and Nightingale, McDonald, and Becker[40] give $\delta=-0.09\pm 0.05$. The recent work of Pilt *et al.*[32] reports $\delta=-(1.0^{+0.02}_{-0.03})$.

For the 4.74-MeV level, we are unable to distinguish between the alternative spin assignments $J=\frac{5}{2}$ or $\frac{9}{2}$. The angular correlation of the 4.74 → 2.03 transition measured at $E_\alpha=6.2$ MeV together with the χ^2 curves resulting from analysis of the 4.74 → 2.03 transition at bombarding energies $E_\alpha=5.8$, 6.0, and 6.2 MeV are illustrated in Fig. 6. The $J=\frac{7}{2}$ alternative is rejected at beyond the 1% confidence limit; the solutions at the minimum in χ^2 also result in $P(\frac{3}{2})>50\%$. If the level has spin $J=\frac{9}{2}$, then for the multipole mixing of the 4.74 → 2.03 transition we find $\tan^{-1}\delta=+(2.0\pm 0.25)^\circ$, while for the $J=\frac{5}{2}$ alternative $\tan^{-1}\delta=-(61\pm 0.5)^\circ$. In either case the transition is mostly quadrupole. The level parity has been suggested to be $\pi=(+1)$ as a result of the direct-reaction work[10]; the results reported here also suggest $\pi=(+1)$. To see this, combine the measured mean life $\tau_m=0.45\pm 0.10\times 10^{-13}$ sec with the γ-ray branching ratio 94% and alternative mixing ratios given above for the 4.74 → 2.03 transition. For $\pi=-1$, this results in $|M(M2)|^2=430$ and 564 W.u. for the $\frac{5}{2}$ and $\frac{9}{2}$ alternatives, respectively. We might expect to be able to choose between the $\frac{5}{2}^+$ and $\frac{9}{2}^+$ alternative assignments by examination of the γ-ray branching ratios to see if any states with spins $\leq\frac{3}{2}$ are populated; we see that this level has no transition to a state with $J\leq\frac{3}{2}$ and so we suggest the $\frac{9}{2}$ alternative. The $J^\pi=\frac{9}{2}^+$ assignment suggested here has been confirmed by the recent experiment of Pilt, Spear, Elliot, and Kuehner.[32] They measured the angular correlation and linear polarization of the 4.74 → 2.03 transition and deduced $J^\pi(4.74)=\frac{9}{2}^+$.

An identical argument applies to the 5.65-MeV level. The angular correlation of the 5.65 → 3.07-MeV transition has the same (within experimental error) Legendre expansion coefficients as the 4.74 → 2.03 transition, and for both transitions the final-

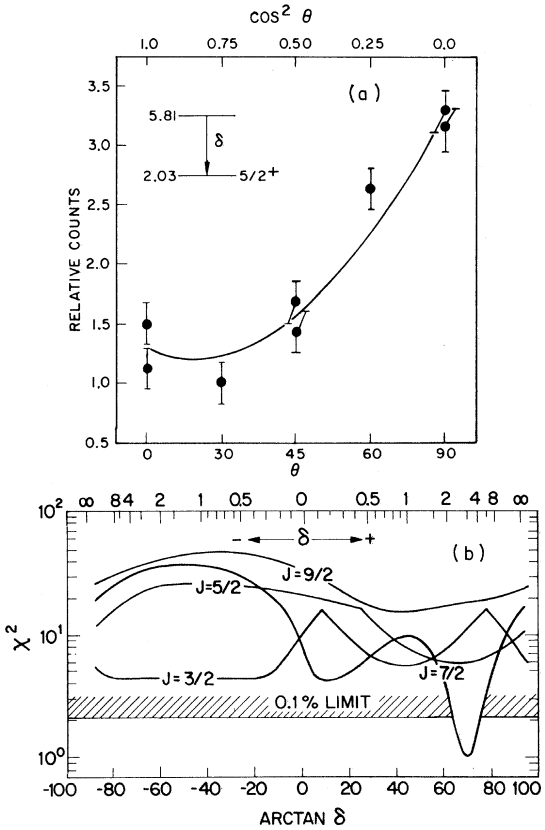

FIG. 5. (a) The angular correlation of the 5.81 → 2.03-MeV transition measured at $E_\alpha=7.2$ MeV. (b) Curves of χ^2 vs arctanδ(5.81 → 2.03) resulting from the combination of individual fits to the angular correlations of the 5.81 → 2.03 transition. These were measured at α bombarding energies $E_\alpha=7.2$, 7.4, and 7.6 MeV.

state spin is the same. Similarly, analysis of the angular correlation of the 5.65 → 3.07 transition results in alternative assignments for the 5.65-MeV level of $J=\frac{5}{2}$ or $\frac{9}{2}$, with $\tan^{-1}\delta(5.65\rightarrow 3.07)=-(62\pm 1.5)^\circ$ and $\tan^{-1}\delta=(3\pm 1)^\circ$, respectively. Here the $\frac{7}{2}$ alternative is not excluded quite as well statistically, but still corresponds to $P(\frac{3}{2})>50\%$. We also made a simultaneous fit to this correlation and that of the 5.65 → 4.08 transition. This results in two alternative values for $\delta(5.65\rightarrow 4.08)$: For $J=\frac{5}{2}$, $\tan^{-1}\delta=+(19\pm 3)$ and $+(62.5\pm 3)$; and for $J=\frac{9}{2}$, $\tan^{-1}\delta=-(17.5\pm 1.5)^\circ$. γ-ray-branching arguments suggest the $J=\frac{9}{2}$ alternative, since no transition is observed from the 5.65-MeV level to a state with $J\leq\frac{3}{2}$. Meyer-Schützmeister *et al.* observe $L_D=2$ in the (He^3,p) reaction and suggest $\pi=(+1)$. For a $\frac{9}{2}^+$ assignment, we would expect the 5.65 → 3.07 transition to be pure $E2$; consistent with this, we find $\tan^{-1}\delta(5.65\rightarrow 3.07)=+(3\pm 1)^\circ$.

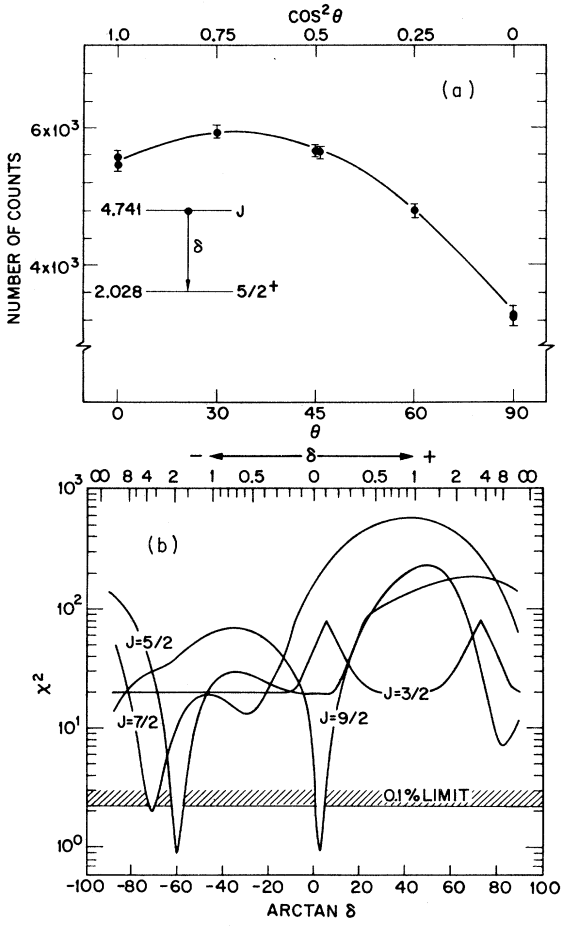

FIG. 6. (a) The angular correlation of the 4.74 → 2.03-MeV transition measured at $E_\alpha=6.2$ MeV. (b) Curves of χ^2 vs arctanδ(4.74 → 2.03) resulting from a combination of individual fits to the angular correlations of the 4.74 → 2.03 transition measured at $E_\alpha=5.8$, 6.0, and 6.2 MeV.

Meyer-Schützmeister *et al.*[10] have suggested that the 4.74- and 5.65-MeV levels might have $J=\frac{1}{2}$, based on the observation that in the $Al^{27}(He^3,p)Si^{29}$ reaction the proton angular distributions resulting in formation of the ground state and the states at 4.74- and 5.65-MeV have a pattern characteristic of orbital angular momentum transfer $L_D=2$ and are produced with the same cross section. Since the ground state has spin $\frac{1}{2}$, they suggest (1) that the observed angular distribution is a prototype of $L=2$ transfers, and (2) a likely assignment for both the 4.74- and 5.65-MeV levels is $J=\frac{1}{2}$. It is clear from our results that the hypothesis (2) is wrong for both levels. The fact that 4.74- and 5.65-MeV levels have spin other than $J=\frac{1}{2}$ is not surprising; these tentative assignments of Ref. 10 were based on the similarity of the cross section and the orbital angular momentum transfer.

The 4.84-MeV level has $J^\pi=\frac{1}{2}^+$, resulting from observation of orbital angular momentum transfer $l_n=0$ in the $Si^{28}(d,p)Si^{29}$ reaction.[33] We measure an isotropic angular correlation for the 4.84 → 0 transition, analysis of which limits J to either $\frac{1}{2}$ or $\frac{3}{2}$; this is consistent with the $J=\frac{1}{2}$ assignment.

The 5.28-MeV level is given the alternative spin assignments $J=\frac{3}{2}$ or $\frac{7}{2}$ based on the analysis of the correlations of the 5.28 → 2.03 transition measured at $E_\alpha=6.4$ and 6.6 MeV. Both solutions require quadrupole-dipole mixing: For $J=\frac{3}{2}$, we have $-79\leq\tan^{-1}\delta(5.28\rightarrow 2.03)\leq -28^\circ$, while for the $\frac{7}{2}$ alternative, $+7\leq\tan^{-1}\delta\leq+28^\circ$. A second solution for $J=\frac{7}{2}$, $\tan^{-1}\delta=(60.5\pm 1)^\circ$, is barely acceptable at the 0.1% confidence level and does not satisfy the population-parameter requirement. The other γ ray from this level, the 5.28 → 1.27 transition, did not have enough intensity at these bombarding energies ($E_\alpha=6.4$ and 6.6 MeV) to permit the extraction of a reliable angular correlation. The γ ray did, however, appear prominently in the spectrum at both $E_\alpha=7.2$ and 7.4 MeV and an angular correlation was obtained at these energies. The Legendre expansion coefficients are listed in Table IV. An analysis of this correlation results in solutions for $J=\frac{5}{2}$ and $\frac{7}{2}$, with the $\frac{3}{2}$ alternative rejected at the 1% confidence level. For the $\frac{7}{2}$ alternative, $\tan^{-1}\delta(5.28\rightarrow 1.27)=-(1.5\pm 1.0)^\circ$ or $+(76\pm 2)^\circ$. Because this last distribution was measured considerably above threshold, our restriction $|m|\leq\frac{3}{2}$ is not valid and so we are reluctant to use the analysis of this correlation to eliminate the $\frac{3}{2}$ alternative assignment. Meyer-Schützmeister *et al.*[10] suggest $\pi=(+1)$ for this level, which is also suggested by the observed multipole mixing of the 5.28 → 2.03 transition, together with the lifetime limit. We list the 5.28-MeV level as $J=\frac{3}{2}$ or $\frac{7}{2}$, $\pi=(+1)$. Pilt *et al.*[32] have reached similar conclusions.

We consider now the levels with $E_x > 6$ MeV. For the 6.11-MeV level, angular correlations were measured for both the $6.11 \rightarrow 2.43$ transition, which restricts $J(6.11) = \frac{3}{2}$ or $\frac{5}{2}$, and the $6.11 \rightarrow 2.03$ transition, which had solutions for all $J > \frac{1}{2}$. For both transitions, the mixing ratios are restricted only within rather broad limits which will be set down in the summary table. There is a report that this state is populated via an $l_n = 1$ (2) transfer in the $Si^{28}(d,p)Si^{29}$ reaction at $E_d = 6.25$ MeV.[36] Our results throw some doubt on the $l_n = 1$ assignment, since this result combined with the restriction $J = \frac{3}{2}$ or $\frac{5}{2}$ given above leads to a $J^\pi = \frac{3}{2}^-$ assignment for the 6.11-MeV level. We then expect both the $6.11 \rightarrow 2.03$ and the $6.11 \rightarrow 2.43$ transitions to have multipolarity $E1$ and mixing ratio $\delta = 0$. However, although $\delta = 0$ is included as a solution in the χ^2 curves for the $6.11 \rightarrow 2.43$ transition (for $J = \frac{3}{2}$), $\delta = 0$ is not allowed for the $6.11 \rightarrow 2.03$ transition where the possible mixing ratios are $-\infty \leq \tan^{-1}\delta \leq -10°$, $20° \leq \tan^{-1}\delta \leq 53°$, and $\tan^{-1}\delta > 88°$. There is some evidence, on the other hand, that the state has $\pi = (+1)$.[10] We thus arrive at $J^\pi(6.11) = \frac{3}{2}^{(+)}, \frac{5}{2}^{(+)}$.

For the 6.19-MeV level, the analysis of the angular correlation of the $6.19 \rightarrow 2.03$ transition permits $J = \frac{3}{2}$, $\frac{5}{2}$, or $\frac{7}{2}$. This is consistent with, but less restrictive than the direct-reaction results; the level is populated with an $l_n = 3$ transition in the $Si^{28}(d,p)Si^{29}$ reaction, thus $J^\pi(6.19) = \frac{5}{2}^-$ or $\frac{7}{2}^-$.[35] Only for the $\frac{7}{2}$ alternative does the mixing ratio of the $6.19 \rightarrow 2.03$ transition include the value $\delta = 0$; we have for the $\frac{7}{2}$ alternative $-5 \leq \tan^{-1}\delta \leq 0°$, while for the $\frac{5}{2}$ alternative $\tan^{-1}\delta = +(37.5 \pm 2.5)°$ or $\tan^{-1}\delta = +(82 \pm 5)°$. [A second solution exists for $J = \frac{7}{2}$, $\tan^{-1}\delta = +(76.5 \pm 1.5)°$, which is rejected since it does not satisfy the population-parameter requirement.] Thus we favor the $\frac{7}{2}$ alternative and assign the 6.19-MeV level $J^\pi = (\frac{7}{2})^-$. The 6.38-MeV level is known to be $J^\pi = \frac{1}{2}^-$ from previous work. It is populated strongly in the γ-ray cascade following slow-neutron capture,[34] and the angular correlation of the $C \rightarrow 6.38 \rightarrow 0$ cascades results in a $J = \frac{1}{2}$ assignment. The level is also populated via a $l_n = 1$ transition in the $Si^{28}(d,p)Si^{29}$ reaction. The angular distribution measured here for the $6.38 \rightarrow 0$ transition is isotropic as expected.

To conclude this section, we summarize the spin assignments and γ-ray multipole mixtures for the levels of Si^{29} for $4.08 \leq E_x \leq 6.38$ MeV in Table VI. We have presented the J^π assignments in three columns: those arising from this work alone [still with the restriction $P(\frac{1}{2}) \geq 50\%$], those previously known, and those we may deduce from a combination of these reports. These data will be presented in a combined form later in the paper.

We note that if one uses the optical model to obtain transmission coefficients and assumes the compound-nucleus model, then one can predict the magnetic-substate populations of the residual nucleus and the γ-ray angular correlations. Comparison of these predictions with the measured angular correlations then may be used to deduce level spins and γ-ray multipole mixing. Hauser-Feshbach[41] calculations are in progress for these data. Initial calculations were done for the 4.74-, 5.28-, and 5.65-MeV levels, where alternative spin assignments result from our work. These calculations give $J = \frac{9}{2}$, $\frac{7}{2}$, and $\frac{9}{2}$ for the 4.74-, 5.28-, and 5.65-MeV levels. The details of these calculations will be described in a future publication.[42] Because these calculations will give a much more reliable measure of the multipole mixing than we can obtain with our simpler estimates of the $P(M's)$, we have quoted multipole mixtures only when our analysis in terms of two population parameters gives a unique result; and we will await the outcome of the Hauser-Feshbach calculation to quote multipole mixtures for those transitions for which we would have to assume the population parameters; for these we give only limits at present.

IV. NUCLEAR LIFETIMES IN Si^{29}

A. Doppler-Shift-Attenuation Measurements

Using Ge(Li) detectors, the measurement of nuclear lifetimes by the Doppler-shift-attenuation technique has become a valuable tool for probing nuclear structure.[12] If deexcitation γ rays are observed from a nuclear level excited in the reaction $A(a,b)B^*$, the mean nuclear lifetime τ_m can be extracted from a measurement of the quantity F_m defined by

$$F_m(\tau_m) = (\Delta E_\gamma)/(\Delta E_{\gamma 0}), \tag{3}$$

where ΔE_γ is the attenuated Doppler shift (recoil into a dense medium) and $\Delta E_{\gamma 0}$ is the full Doppler shift (recoil into vacuum). A number of variants of the method have been employed. The one used here was first used by Warburton, Alburger, and Wilkinson[43] and involves the measurement of ΔE_γ for two materials having different characteristic stopping times. We may write

$$R(\tau_m) = \frac{[F_m(\tau_m)]_1}{[F_m(\tau_m)]_2} = \frac{(\Delta E_\gamma)_1}{(\Delta E_\gamma)_2}. \tag{4}$$

The calculated value of $R(\tau_m)$ is almost independent of $\Delta E_{\gamma 0}$ if the reaction kinematics insure that all nuclei recoil forward into the target, so the necessity of calculating or measuring the "vacuum shift" $\Delta E_{\gamma 0}$ is avoided. The method lends itself naturally to the use of homogeneous targets (alloys, compounds, or elemental substances) which eliminates corrections for target thickness and simplifies the

TABLE VI. Level spin and γ-ray multipole-mixing ratios deduced from the γ-ray angular correlations listed in Table IV. The error quoted for the multipole mixing consists of the statistical error compounded with a $\tan^{-1} 2°$ systematic error. The mixing ratio for the transition $E_i \rightarrow E_f$ is quoted as $\delta(E_f)$.

E_x (MeV)	J^π Ref. a	Ref. b	Ref. c	$\delta(0)$	$\delta(1.27)$	$\delta(2.03)$	$\delta(2.43)$	$\delta(3.07)$	$\delta(3.62)$	$\delta(4.08)$
4.08	$\frac{5}{2}$ [d]				-1.73 ± 0.32 [d]					
	$\frac{7}{2}$	$\frac{7}{2}^+$	$\frac{7}{2}^+$		$+0.023 \pm 0.04$	-0.14 ± 0.04				
4.74	$\frac{5}{2}$					-1.80 ± 0.15				
	$\frac{7}{2}$ [d]									
	$\frac{9}{2}$	$\frac{9}{2}^+$	$\frac{9}{2}^+$			$+0.035 \pm 0.035$				
4.84	$\frac{1}{2}$	$\frac{1}{2}^+$	$\frac{1}{2}^+$	(0)						
	$\frac{3}{2}$			...						
4.90	$\frac{5}{2}$	$(\frac{5}{2})^+$	$\frac{5}{2}^+$	$+0.017 \pm 0.044$	-0.035 ± 0.038	$+0.035 \pm 0.067$				
4.93	$\frac{3}{2}$	$\frac{3}{2}^-$	$\frac{3}{2}^-$	...						
5.25	$\frac{9}{2}^{(-)}$		$\frac{9}{2}^{(-)}$						-0.49 ± 0.07 -2.41 ± 0.30 [d]	
5.28	$\frac{3}{2}$					$-6.3 \leq \delta \leq -0.49$				
	$\frac{7}{2}$	$\frac{7}{2}^{(+)}$	$\frac{7}{2}^{(+)}$		-0.026 ± 0.039 $+4.01 \pm 0.88$	$0.09 \leq \delta \leq 0.58$ 1.76 ± 0.20 [d]				
5.65	$\frac{5}{2}$							-1.88 ± 0.20		$+0.344 \pm 0.070$ -1.92 ± 0.28
	$\frac{7}{2}$ [d]									
	$\frac{9}{2}$	$\frac{9}{2}^{(+)}$	$\frac{9}{2}^{(+)}$					$+0.052 \pm 0.039$		-0.315 ± 0.043
5.81	$\frac{7}{2}^{(+)}$		$\frac{7}{2}^{(+)}$			$+2.19 \pm 0.23$				
5.95	$\frac{3}{2}$	$(\frac{3}{2}, \frac{5}{2})^+$	$\frac{3}{2}^+$	...						
6.11	$\frac{3}{2}$	(+)	$\frac{3}{2}^{(+)}, \frac{5}{2}^{(+)}$			...	...			
	$\frac{5}{2}$					...	...			
6.19	$\frac{3}{2}$					...				
	$\frac{5}{2}$	$(\frac{5}{2}, \frac{7}{2})^-$				$+0.767 \pm 0.089$ $+7.11^{+12.0}_{-2.8}$				
	$\frac{7}{2}$		$\frac{7}{2}^-$			$-0.12 < \delta < +0.03$ $+4.17 \pm 0.85$ [d]				

TABLE VI (*Continued*)

E_x (MeV)	J^π Ref. a	Ref. b	Ref. c	δ(0)	δ(1.27)	δ(2.03)	δ(2.43)	δ(3.07)	δ(3.62)	δ(4.08)
6.38	$\frac{1}{2}$	$\frac{1}{2}^-$	$\frac{1}{2}^-$	...						
	$\frac{3}{2}$			...						

[a] Deduced from the angular correlations and lifetime measurements reported in this experiment only.

[b] Other measurements.

[c] Deduced from the available experimental evidence, as described in the text.

[d] Rejected because $P(\frac{1}{2})/P(\frac{3}{2})<1.0$.

[e] In Ref. 36 observation of an $l_n=1$ transfer in the $Si^{28}(d,p)Si^{29}$ reaction is reported, which would result in $\pi=-1$. See the discussion in the text.

measurement of very fast lifetimes.

Two conditions make the preceding technique ideal for the study of lifetimes in Si^{29} by the Mg^{26}-$(\alpha, n)Si^{29}$ reaction. The beam energy can be chosen just above threshold for the production of the nuclear level being studied confining the recoils to a narrow forward cone and insuring that all recoils stop in the target. Pure magnesium has a very long characteristic stopping time and alloys readily with gold to form a medium with a short characteristic stopping time. The following simple technique was used to make the magnesium-gold alloy: Gold foil and Mg^{26} foil were wrapped together and melted in vacuum by electron beam heating. A concentration of 10% Mg^{26} atoms by number resulted in an alloy with a measured density of 16.0 g/cm^3 which was cold-rolled to thickness 5–15 mg/cm^2 for use as a target.

The distribution of magnesium throughout the alloy was checked by scanning a cross section of the foil with an electron microprobe. The magnesium concentration varied between 7 and 13%, a variation which probably resulted from unequal heating by the electron beam during fabrication. Since magnesium is completely soluble in gold up to a concentration of 20 at.%, there were no small-scale nonuniformities in the characteristic stopping power of the alloy.[44]

For the lifetime measurements, ΔE_γ was determined from two runs at a forward and backward angle. The beam energy for the $Mg^{26}(\alpha, n)Si^{29}$ reaction was chosen 0.5 to 1.0 MeV above threshold except in the case of the 1.27- and 2.03-MeV levels where considerations of yield required a bombarding energy >4 MeV above threshold. Suitable standard sources were used to monitor the gain of the Ge(Li) detector system, and corrections for gain shifts were usually smaller than statistical uncertainties. The experimental results for ΔE_γ are presented in Table VII. Figures 7 through 9 illustrate line-shape fits to the data.

The lifetimes were extracted using the energy-loss theory of Lindhard, Scharff, and Schiøtt.[45] A computer code was used to evaluate $F_m(\tau_m)$ from the expression

$$F_m(\tau_m)=\frac{1}{v_i\tau_m}\int_0^\infty v(t)\cos\varphi e^{-t/\tau_m}dt, \qquad (5)$$

where v_i is the initial recoil velocity and $\cos\varphi$ is the nuclear scattering correction which has been evaluated by Blaugrund.[46] The small spread in initial recoil velocities was neglected in the calculation of $F_m(\tau_m)$. Values adopted for the energy-loss parameters are given in Table VII. The value $f_e=0.92$ is suggested by the data of Ormrod and Duckworth[47] for Si^{29} ions stopping in carbon. Values for f_n were obtained by fitting the line shape of the

2.03-MeV γ ray.

In all cases except the long-lived 3.62-MeV level, lifetimes were determined from the ratio $R(\tau_m)$ (column 9 of Table VIII). For the 3.62-MeV level, it is preferable to rely on the calculated value of $\Delta E_{\gamma 0}$ and use F_m(Mg). Final values for τ_m are listed in column 10 of Table VII. To obtain the very fast lifetime for the 4.90-MeV level, the γ rays from the full-energy, one- and two-escape peaks of the 4.93 → 0 transition were used as reference standards. The lifetime of the 4.93-MeV level has been measured by resonance fluorescence to be 1.16 fsec.[48] The value quoted here for the mean life of the 5.25-MeV level, $\tau_m = 100 \pm 20$ psec, is to be preferred over the value reported earlier, $\tau_m = 95 \pm 15$ psec.[13] The uncertain knowledge of the energy-loss parameters has been taken into account by combining an arbitrary 15% additional uncertainty with the statistical uncertainty in the centroid determinations.

In principle, greater statistical precision is possible if one fits the experimental spectrum with a calculated line shape to determine τ_m, and various techniques have been described for performing this type of fit.[49-51] However, the centroid analysis based on Eq. (5) is easier to standardize and improved statistical precision is not of much value when the uncertainty in the energy-loss parameters is as large as 15%. We have therefore based our final lifetimes on the centroid analysis. Typical line-shape fits are presented in Figs. 7–9 and serve to check the internal consistency of the measurements. The fitting program described by Fisher *et al.*,[51] modified to include the nuclear scattering correction of Blaugrund,[46] was used in performing the fits. A detailed description of this program, which runs on a small computer with 8000 units of

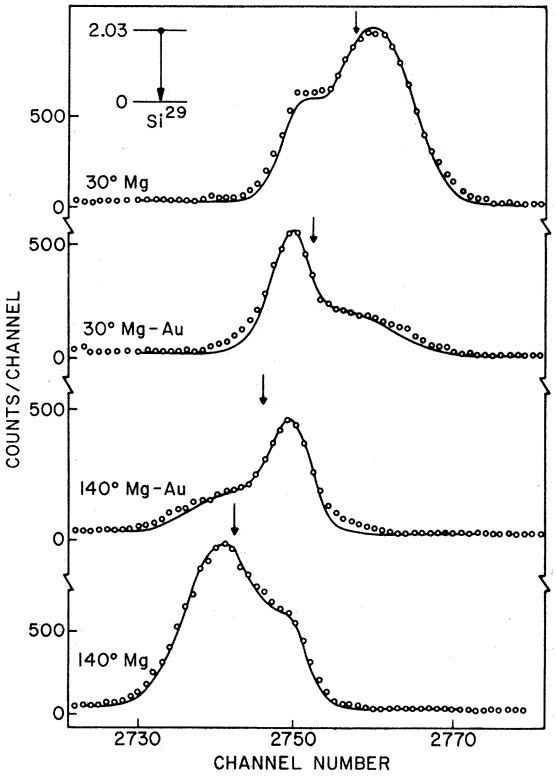

FIG. 7. Portions of the γ-ray pulse-height distributions obtained when foils of either Mg^{26} or Mg^{26}-Au alloy are bombarded with 4.0-MeV α particles. The peaks in all four spectra correspond to the Si^{29} 2.03 → 0-MeV transition, observed at either $\theta_\gamma = 30$ or 140° for the alternate targets. The vertical arrows indicate the centroid of the peak distributions obtained after background subtraction. The Doppler-shift attenuations F for the Mg^{26} foil vs the Mg^{26}-Au foil targets are quite different: F(Mg-Au)/F(Mg) = 0.41 ± 0.02. The smooth line drawn through the curve represents the line shape calculated for this transition with the parameters described in the text.

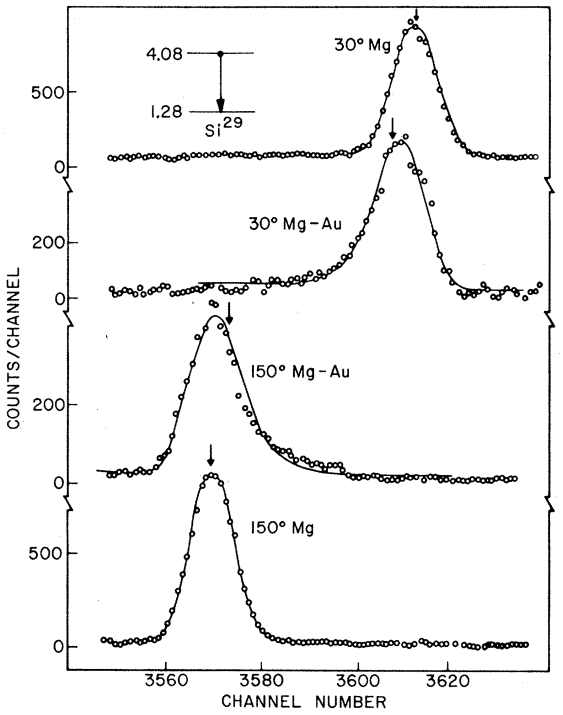

FIG. 8. Portions of the γ-ray pulse-height distribution obtained when foils of either Mg^{26} or Mg^{26}-Au alloy are bombarded with 5.8-MeV α particles. The peaks in all four spectra correspond to the Si^{29} 4.08 → 1.27-MeV transition, observed at either $\theta_\gamma = 30$ or 150° for the alternative targets. The centroid of the peaks remaining after background subtraction is indicated by the vertical arrow. The ratio of the Doppler-shift attenuations for the γ ray is F_m(Mg-Au)/F_m(Mg) = 0.83 ± 0.01. The smooth curves through these data represent the line shapes calculated for this transition with the parameters described in the text.

TABLE VII. Energy-loss parameters for stopping of Si^{29} ions in gold and magnesium. α_e is the characteristic stopping time defined by $Mc/(137K_e)=\alpha_e$. The quantities f_e, f_n, and K_e are defined by Lindhard, Scharff, and Schiøtt (Ref. 45).

Stopping medium	f_e	f_n	f_eK_e (keV cm²/μg)	α_e (sec)
Mg^{26}	0.92	2.0	2.84	1.33×10^{-12}
Au^{197}	0.92	1.0	0.78	4.4×10^{-13}
10% Mg^{26} 90% Au^{197} $\rho=16.0$ gm/cm³			0.81	5.1×10^{-13}

memory storage, is available on request.

Line-shape fitting of the deexcitation γ rays from the 2.03-MeV level was used to establish the values of f_n for Si^{29} ions in gold and magnesium. It is not always possible to make an independent determination of f_n and τ_m in a line-shape fit, since the χ^2 minimum in the two-parameter space may be extremely shallow, but in favorable cases this can be accomplished.[50] The magnesium and magnesium-gold alloy measurements were combined, and the total χ^2 was minimized as a function of three parameters: τ_m, f_n(Mg), and f_n(Au). The minimum χ^2 was achieved for a mean life 400 ± 70 fsec and values 2.0 ± 0.5 and 1.0 ± 0.3 for f_n(Mg) and f_n(Au), respectively. The uncertainties in the val-

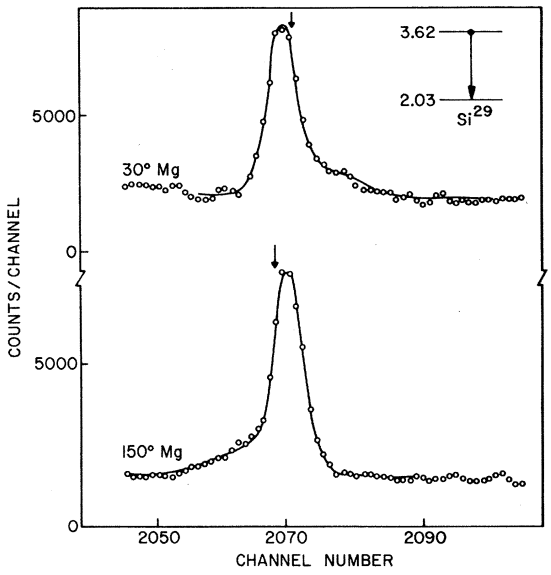

FIG. 9. Portions of the γ-ray spectra are obtained when a Mg^{26} foil target is bombarded by 5.1-MeV α particles, observed at $\theta_\gamma=30$ and 150°. The peak corresponds to the full-energy-loss peak of the 3.62→2.03-MeV transition. The vertical arrows indicate the peak centroid after background subtraction. The observed Doppler shift $E_\gamma(0°)-E_\gamma(180°)$ deduced from these spectra is $F_m(\mathrm{Mg})=0.105\pm0.01$. The smooth curves through these data represent the line shapes calculated with the parameters given in the text.

TABLE VIII. Summary of experimental results for ^{29}Si lifetimes. Values for ΔE_γ refer to the quantity $E_\gamma(0°)-E_\gamma(180°)$.

E_x (MeV)	E_γ (MeV)	$\bar{E}_\alpha$ (MeV)	ΔE_γ(Mg) (keV)	ΔE_γ(Mg-Au) (keV)	ΔE [a] (keV)	F_m(Mg)	F_m(Mg-Au)	R [b]	τ_m (fsec)
1.27	1.27	4.0	9.20 ± 0.15	3.76 ± 0.15	15.4	0.60	0.25	0.41 ± 0.02	360 ± 70
2.03	2.03	4.0	14.7 ± 0.15	5.95 ± 0.20	24.6	0.60	0.25	0.41 ± 0.02	360 ± 70
2.43	2.43	4.0	28.6 ± 0.20	26.8 ± 0.20	29.4	0.98	0.91	0.94 ± 0.01	13 ± 3
3.07	1.79	4.0	21.4 ± 0.50	19.3 ± 0.50	21.7	0.99	0.89	0.90 ± 0.03	20 ± 7
3.62	1.60	5.1	2.30 ± 0.22	···	21.9	0.105 ± 0.01	···		4000 ± 800
4.08	2.81	5.8	40.0 ± 0.30	32.2 ± 0.60	41.0	0.98	0.81	0.83 ± 0.01	48 ± 8
4.74	2.71	5.8	38.0 ± 0.20	32.0 ± 0.60	39.5	0.96	0.81	0.84 ± 0.02	45 ± 10
4.84	4.84	6.6	···	···	···	···	···	0.99 ± 0.01	<5 [c]
4.90	4.90	6.6	···	···	···	···	···	0.96 ± 0.01	10 ± 3 [c]
4.93	4.93	6.6	···	···	···	···	···	1.02 ± 0.04	<10
5.25	1.63	6.6	24.2 ± 0.30	17.2 ± 0.70	25.4	0.95	0.68	0.71 ± 0.03	100 ± 20
5.28	3.26	6.6	···	···	···	···	···	1.02 ± 0.04	<10
5.65	2.59	7.2	39.0 ± 1.2	34.6 ± 1.2	39.5	0.99	0.88	0.89 ± 0.04	40 ± 15
	1.57	7.2	23.4 ± 1.2	23.4 ± 1.2	23.9	1.19	0.98	0.84 ± 0.06	
5.81	3.78	7.2	···	···	···	···	···	0.98 ± 0.04	<20
5.95	5.95	7.2	···	···	···	···	···	0.95 ± 0.06	<30
6.11	4.08	7.2	···	···	···	···	···	1.02 ± 0.03	<8
6.19	4.16	7.2	···	···	···	···	···	0.99 ± 0.04	<15

[a] Calculated by assuming anisotropic angular distribution for recoils in the center-of-mass system.

[b] $R=\Delta E_\gamma(\mathrm{Mg\text{-}Au})/\Delta E_\gamma(\mathrm{Mg})$. The individual shifts ΔE_γ(Mg-Au) and ΔE_γ(Mg) involve systematic uncertainties not present in the ratio R. The individual shifts are given only for cases in which an actual lifetime, rather than an upper limit, was obtained.

[c] 4.93-MeV line used as reference standard.

ues of f_n are correlated, and the ratio of these values is fixed more accurately: $f_n(\mathrm{Mg})/f_n(\mathrm{Au}) = 2.0 \pm 0.1$. This figure is consistent with the recent results of Currie, Earwaker, and Martin.[49]

A comparison between the present results and recent results of other groups[52, 53] is shown in Table IX. The agreement between the results, all obtained with the Doppler-shift technique, is strikingly good. Earlier measurements[54, 55, 9] performed on the 1.27- and 2.03-MeV levels using Coulomb-excitation and resonance-fluorescence techniques show somewhat poorer agreement with the present results. A partial level scheme for Si^{29} incorporating these measurements together with the results of Secs. II and III is presented in Fig. 10.

B. Electromagnetic Decay Properties of Si^{29}

A fairly comprehensive picture of the electromagnetic decay properties of Si^{29} for levels in the region of excitation energy $0 \leq E_x(\mathrm{MeV}) \leq 6.38$ can be constructed by using the lifetimes of these levels, together with γ-ray branching ratios (Table III) and multipole mixing ratios (Table VI). This material is presented in Table X. The partial transition strengths are quoted in Weisskopf units (calculated using a radius constant $r_0 = 1.2$ fm). For each level, the values of the lifetime, γ-ray branching ratio, and multipole mixing used to obtain these transition strengths are also listed. For levels with $E_x < 4.08$ MeV, values for these parameters quoted are from the literature. For levels with $E_x > 4.08$ MeV, branching ratios were determined from a combination of the branching ratios and uncertainties listed in Table III, except that we have disregarded the measurements of Dickens.[26]

TABLE IX. Comparison of lifetime results with those of other investigators. Mean lifetimes are in fsec.

E_x (MeV)	Present experiment	Ref. 52	Ref. 53	Ref. a
1.27	360 ± 70	370^{+60}_{-50}	310^{+110}_{-80}	
2.03	360 ± 70	370^{+70}_{-60}	350^{+90}_{-80}	
2.43	13 ± 3	<46	20 ± 7	
3.07	20 ± 7	<74	23 ± 11	
3.62	4000 ± 800	4800^{+3000}_{-1500}		3900 ± 500
4.08	48 ± 8	70 ± 20		
4.74	45 ± 10			
4.84	<5	<13		
4.90	10 ± 3			
4.93	<10			
5.25	100 ± 20			
5.28	<10			
5.65	40 ± 15			
5.81	<20			
5.95	<30			
6.11	<8			
6.19	<15			

[a] A. B. McDonald, T. K. Alexander, O. Haussen, and G. T. Ewan, Bull. Am. Phys. Soc. 15, 565 (1970).

V. DISCUSSION

A. Interpretation of γ-Ray Angular Correlations from Decaying Nuclei Aligned by Bombardment near Threshold

In Sec. II, we gave a discussion of the standard techniques for the analysis of γ-ray angular correlations from aligned nuclei, viz. the Methods I and II of Litherland and Ferguson. We recall that

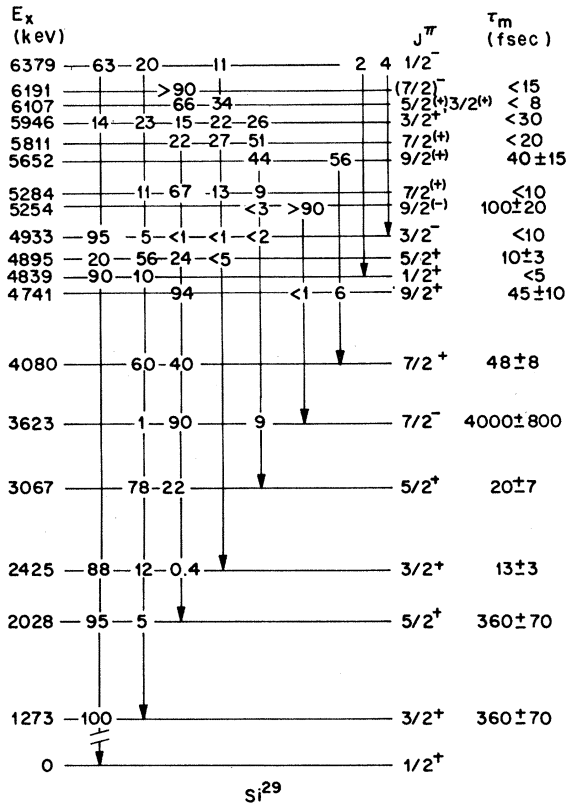

FIG. 10. A partial level scheme for Si^{29}. The excitation energies E_x are from this work. Level spin, parity, and γ-ray decay modes for levels with $E_x \leq 4.08$ MeV are from the literature, while for levels with $E_x > 4.08$ MeV, the values are from both the literature and this experiment.

TABLE X. Electromagnetic decay properties of Si^{29} for states with observed lifetimes, branching ratios, and multipole mixing.

E_x (MeV)	$E_\gamma(E_i \to E_f)$ (MeV)	$J^\pi_i \to J^\pi_f$	τ_m (fsec)	Branch (%)	$\delta\left(\frac{L+1}{L}\right)$ [a]	$\lvert M(L=1)\rvert^2$ [b]	$\lvert M(L=2)\rvert^2$ [b]
1.273	1.273(1.273→0.0)	$\frac{3}{2}^+ \to \frac{1}{2}^+$	360 ± 70	100	−0.20 ± 0.02 [c]	0.041 ± 0.008	4.8 ± 1.3
2.028	2.028(2.028→0.0)	$\frac{5}{2}^+ \to \frac{1}{2}^+$	360 ± 70	95 ± 1	0		11.7 ± 2.3
	0.756(2.028→1.273)	$\frac{5}{2}^+ \to \frac{3}{2}^+$		5 ± 1	(0)	(0.010 ± 0.003)	7.7 ± 4.8
2.425	2.425(2.425→0.0)	$\frac{3}{2}^+ \to \frac{1}{2}^+$	13 ± 3	88 ± 1	+0.26 ± 0.08 [d]	0.14 ± 0.03	
	1.152(2.425→1.273)	$\frac{3}{2}^+ \to \frac{3}{2}^+$		12 ± 1	(0)	(0.19 ± 0.05)	
	0.399(2.425→2.028)	$\frac{3}{2}^+ \to \frac{5}{2}^+$		0.4 ± 0.1 [e]	(0)	(0.15 ± 0.05)	
3.067	1.794(3.067→1.273)	$\frac{5}{2}^+ \to \frac{3}{2}^+$	20 ± 7	79 ± 1	−0.27 ± 0.02 [c]	0.20 ± 0.07	21.7 ± 8.3
	1.039(3.067→2.028)	$\frac{5}{2}^+ \to \frac{5}{2}^+$		21 ± 1	−0.04 ± 0.02 [c]	0.29 ± 0.10	$2.07^{+2.67}_{-1.71}$
3.623	2.351(3.623→1.273)	$\frac{7}{2}^- \to \frac{3}{2}^+$	4000 ± 800	1 ± (0.2) [f]	(0)		(0.16 ± 0.05)
	1.596(3.623→2.028)	$\frac{7}{2}^- \to \frac{5}{2}^+$		90 ± 1	+0.02 ± 0.02	5.7 ± 1.2 × 10^{-5}	
	0.556(3.623→3.067)	$\frac{7}{2}^- \to \frac{5}{2}^+$		9 ± 1	(0)	(1.4 ± 0.3) × 10^{-4}	
4.080	2.806(4.080→1.273)	$\frac{7}{2}^+ \to \frac{3}{2}^+$	48 ± 8	59 ± 1	+0.03 ± 0.03		10.6 ± 1.8
	2.053(4.080→2.028)	$\frac{7}{2}^+ \to \frac{5}{2}^+$		41 ± 1	−0.05 ± 0.02 [c]	0.03 ± 0.01	$0.09^{+0.09}_{-0.06}$
4.741	2.713(4.741→2.028)	$\frac{9}{2}^+ \to \frac{5}{2}^+$	45 ± 10	94 ± 1	+0.04 ± 0.04		21.4 ± 4.8
	0.660(4.741→4.080)	$\frac{9}{2} \to \frac{7}{2}^+$		6 ± 1	(0)	(0.15 ± 0.04)	
4.895	4.895(4.895→0.0)	$\frac{5}{2}^+ \to \frac{1}{2}^+$	10 ± 3	20 ± 1	+0.02 ± 0.04		1.1 ± 0.3
	3.622(4.895→1.273)	$\frac{5}{2}^+ \to \frac{3}{2}^+$		56 ± 3	−0.03 ± 0.04	0.04 ± 0.01	
	2.867(4.895→2.028)	$\frac{5}{2}^+ \to \frac{5}{2}^+$		24 ± 1	+0.04 ± 0.07	0.03 ± 0.01	
4.933	4.933(4.933→0.0)	$\frac{3}{2}^- \to \frac{1}{2}^+$	1.16 ± 0.19 [g]	95 ± 1	(0)	(7.0 ± 1.1 × 10^{-3})	
				5 ± 1	(0)	(0.90 ± 0.23 × 10^{-3})	
5.254	1.631(5.254→3.623)	$\frac{9}{2}^- \to \frac{7}{2}^-$	100 ± 20	100	−0.49 ± 0.07	0.06 ± 0.01	25 ± 8
5.284	4.011(5.284→1.273)	$\frac{7}{2}^+ \to \frac{3}{2}^+$	<10	11 ± 1	(−0.03 ± 0.04)		>1.6 ± 0.2
	3.256(5.824→2.028)	$\frac{7}{2}^+ \to \frac{5}{2}^+$		67 ± 2	$0.09 \le \delta \le 0.50$	>0.04	>0.22
5.652	2.585(5.652→3.067)	$\frac{9}{2}^+ \to \frac{5}{2}^+$	40 ± 15	44 ± 11	+0.05 ± 0.04		14.4 ± 6.5
	1.572(5.652→4.080)	$\frac{9}{2}^+ \to \frac{7}{2}^+$		56 ± 11	−0.31 ± 0.04	0.10 ± 0.04	20.3 ± 10.1
5.811	3.785(5.813→2.028)	$\frac{7}{2}^+ \to \frac{5}{2}^+$	<20	22 ± 3	+2.19 ± 0.23	>1.1 ± 0.2 × 10^{-3}	>1.8 ± 0.2
	3.387(5.813→2.425)	$\frac{7}{2}^+ \to \frac{3}{2}^+$		27 ± 5	(0)		(>4.6 ± 0.9)
6.379	6.379(6.379→0.0)	$\frac{1}{2}^- \to \frac{1}{2}^+$	0.48 ± 0.16	63 ± 1 [i]	(0)	(5.2 ± 1.7 × 10^{-3})	
	5.106(6.379→1.273)	$\frac{1}{2}^- \to \frac{3}{2}^+$		20 ± 2	(0)	(3.2 ± 1.1 × 10^{-3})	
	3.954(6.379→2.425)	$\frac{1}{2}^- \to \frac{3}{2}^+$		11 ± 1	(0)	(3.8 ± 1.3 × 10^{-3})	
	1.540(6.379→4.839)	$\frac{1}{2}^- \to \frac{1}{2}^+$		2 ± 1	(0)	(1.2 ± 0.7 × 10^{-2})	
	1.446(6.379→4.933)	$\frac{1}{2}^- \to \frac{3}{2}^-$		4 ± 2	(0)	(0.9 ± 0.5)	

[a] The multipole mixing ratio. Here the sign convention is given in H. J. Rose and D. M. Brink, Rev. Mod. Phys. 39, 306 (1967).

[b] The transition speed in Weisskopf units.

[c] Reference 31.

[d] A. E. Litherland and G. J. McCallum, Can. J. Phys. 38, 927 (1960).

[e] W. R. Harris, K. Nagatani, and D. E. Alburger, Phys. Rev. 187, 1445 (1969).

[f] T. K. Alexander, private communication.

[g] S. J. Skorka, T. W. Retz-Schmidt, H. Schmidt, J. Morgenstern, and D. Evers, Nucl. Phys. A68, 177 (1965).

[h] Reference 10.

[i] Reference 24.

in Method I, all of the (allowed) magnetic substates of the residual nuclear level may be populated in the reaction and the alignment of the residual decaying nucleus is determined from the γ-ray angular correlations, while in Method II, alignment is obtained by using a special geometry so that magnetic substates which may be populated are limited to those with quantum numbers $|m| \leq J_a + J_b + J_c$, where J_a, J_b, and J_c denote the spins of the target nucleus, projectile, and outgoing light particle, respectively. In this work, we have used another method for producing alignment, i.e., bombardment near threshold with the (α, n) reaction, and we have relied on the great difference in penetrabilities for outgoing s-, p-, and d-wave neutrons to produce alignment of the residual nucleus. We expect $P(\frac{1}{2}) > P(\frac{3}{2}) > P(\frac{5}{2})\ldots$, i.e., the outgoing neutrons will be primarily s wave, with some smaller p-wave contribution, and smaller still d-wave contribution, etc. These population parameters may be estimated from neutron penetrabilities, and more precisely from transmission coefficients obtained from optical-model calculations. These considerations lead to the upper limit, $P(\frac{1}{2}) > 50\%$, used in Sec. III to choose between alternative spin assignments and multipole mixtures.

If we recall Sec. III and examine Table VI, we see that in general, this technique works well for measuring a level spin, and not so well for measuring γ-ray multipole mixing ratios. Of the 13 known states in the excitation-energy interval, $4.08 \leq E_x \leq 6.38$, definite spin assignments have been made to 6 and alternative assignments to 7; quite a few γ-ray multipole mixings have also been deduced. The total information deduced from these results is just about that which would be obtained from analysis of the angular correlations measured in the p-γ coincidence experiment in the

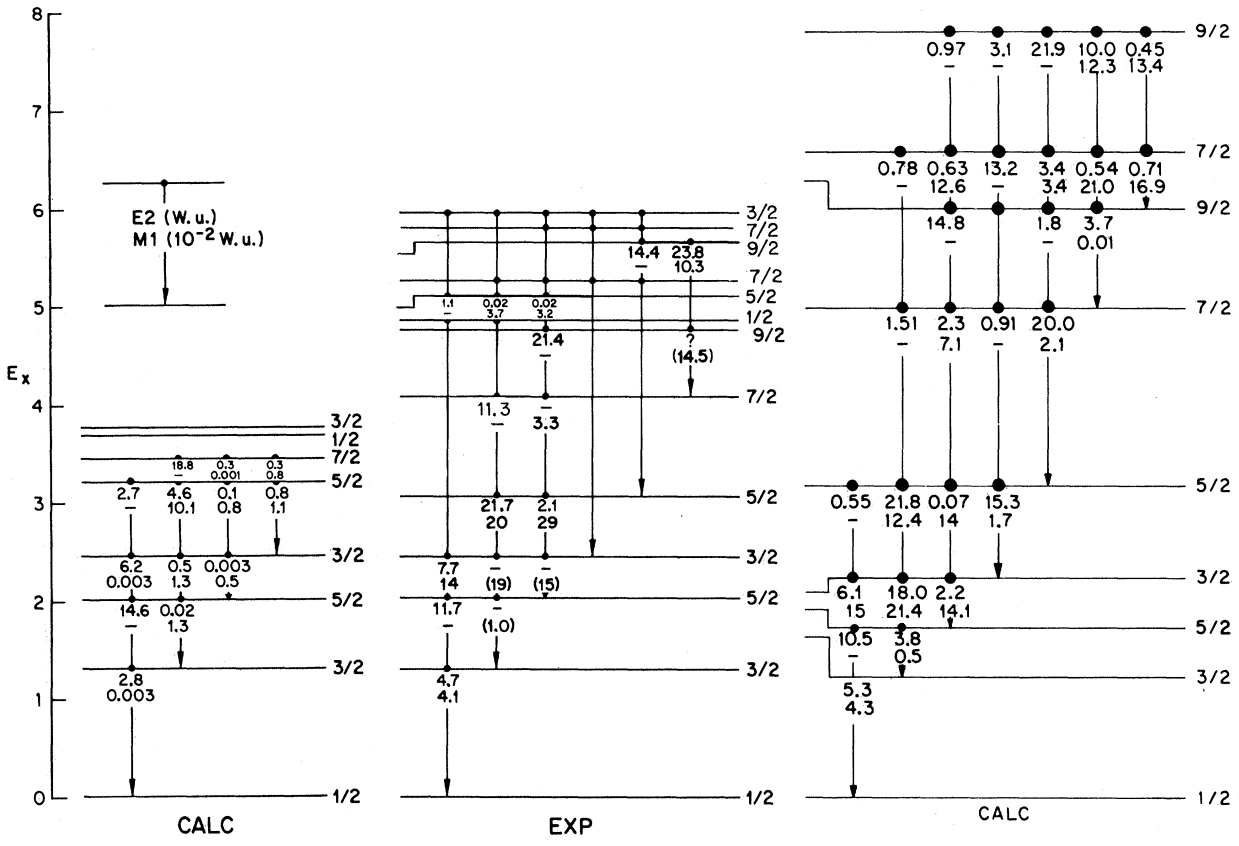

FIG. 11. A comparison of the predictions of nuclear models and experiment for the positive-parity levels of Si^{29}. Both level energy and transition rates are compared; excitation energies may be obtained from the scale at the left, while transition rates are included by insetting the vertical line indicating a γ-ray transition with the $E2$ rate (in Weisskopf units) above the $M1$ rate (in 10^{-2} Weisskopf units). In some cases $M1$ transition rates are calculated with an assumed mixing ratio $\delta = 0$; these are enclosed in parentheses. The calculated spectrum at the left represents the predictions of a modified intermediate-coupling model (Ref. 4) while that on the right is the result of a band-mixing calculation (Ref. 57).

Method II geometry which results in the same restriction on the magnetic quantum numbers of the residual nucleus, $|m| \leq \frac{3}{2}$ (e.g., the $Si^{28}(d,p\gamma)Si^{29}$ reaction) and not as good as that which would be obtained if the γ rays had been detected in coincidence with neutrons detected near 0° in the present experiment [the $Mg^{26}(\alpha, n\gamma)Si^{29}$ reaction], which would result in the limit $|m| \leq \frac{1}{2}$. Conclusions based on this last technique, however, are independent of any assumptions about the reaction mechanism or *ad hoc* restrictions on the magnetic-substate populations. We feel, however, that the technique employed here which requires singles measurements is quite useful as long as the reaction proceeds predominantly by outgoing s-wave neutrons. This means that: (1) the state must be produced with a cross section about that expected for the compound-nucleus process; and (2) the bombarding energy must be close to the threshold energy, conditions which can be checked by excitation function measurements and cross-section measurements for the levels involved.

More restrictions on the spin alternatives and especially on the γ-ray multipole mixtures can be placed if a definite reaction mechanism and nuclear model are invoked, in which case the $P(m)$'s may be directly calculated. The appropriate model here is the compound-nucleus picture. If one assumes the Hauser-Feshbach conditions, i.e., that there is averaging over many levels in the compound system, and $\Gamma/D > 1$, then the angular correlations and cross sections may be compared with the measurements described here. A detailed description of these results will be given elsewhere.[42]

B. Comparison with Nuclear-Model Calculations for Positive-Parity Levels

No attempts to describe the properties of Si^{29} within the framework of the shell model with a large spherical basis have been reported in the literature, due to the large model space required for the calculation. There are, however, predictions of the positive-parity spectra in the framework of (1) an intermediate-coupling model and (2) the strong-coupling model, and it is interesting to compare these predictions with our results.

Intermediate-Coupling Model

Detailed calculations in which a nucleon is coupled to a vibrating even-even core have recently been reported by Bailey and Choudbury,[3] and by Castel, Stewart, and Harvey.[4] In the calculation of Castel, Stewart, and Harvey, the $2d_{3/2}$, $2s_{1/2}$, and $1d_{5/2}$ orbits are available to particle and hole states, while Bailey and Choudbury include just the $d_{3/2}$ and $2s_{1/2}$ orbits for the odd nucleon.

We illustrate in Fig. 11 the results of Castel, Stewart, and Harvey along with the experimental spectra. We see that the $E2$ transition rates are reasonably well reproduced except for the 3.07-MeV level, where the prediction $\Gamma(E2;\ 3.07 \to 0) = 2.7$ W.u. is not in accord with experiment [$\Gamma(E2) < 0.75$ W.u.].[7] We also see that the $M1$ transition rates are not well predicted at all. Note also that the predicted $J = \frac{1}{2}$ and $\frac{3}{2}$ states at 3.75 MeV are quite low in energy if they are to be identified with the 4.839- and 5.946-MeV levels. A more detailed account is given in Ref. 4. A subsequent calculation in which a rotational core is assumed leads to somewhat better agreement with experiment.[56]

Strong-Coupling Model

Bromley, Gore, and Litherland[5] in 1957 concluded that the features (known then) of the low-lying levels of Si^{29} with positive parity could be explained in terms of two noninteracting rotational bands based on (1) the ground state (Nilsson orbit No. 9), and (2) the 1.27-MeV level (Nilsson orbit No.8). The nucleus was characterized by a negative deformation $\eta = -2$. The electromagnetic decay properties of the levels were not well described in terms of this picture, however, and Bromley, Gore, and Litherland suggested that the description might be improved if the two bands were allowed to mix. Hirko[6] has done this calculation for the states with $0 \leq E_x(\text{MeV}) \leq 3.07$, i.e., $J \leq \frac{5}{2}$ with good success, and now has extended it to predict the properties of the $J = \frac{7}{2}$ and $\frac{9}{2}$ states.[57] The parameters of the model were fixed by the excitation energies and electromagnetic decay rates of the states with $E_x \leq 3.07$ MeV, together with the magnetic moment of the ground state. The properties of the $\frac{7}{2}^+$ and $\frac{9}{2}^+$ members of the mixed $K = \frac{1}{2}$ and $\frac{3}{2}$ bands were then predicted. The results of this calculation are illustrated in Fig. 11. We see that the excitation energies of the higher states are not predicted very well; this is to be expected in a calculation which neglects the interaction of other bands at higher energy with the $J = \frac{7}{2}$ and $\frac{9}{2}$ levels. We can compare transition rates for these states except for the upper $\frac{7}{2}^+$ state. The agreement with the electromagnetic transition ratios is quite good; the calculation predicts the known $E2$ and $M1$ transition rates for all states with $J \leq \frac{9}{2}$ within about a factor of 2, which is frequently within the experimental uncertainty. There are two candidates for the second $J = \frac{7}{2}$ state, i.e., the 5.28- and 5.81-MeV levels. The 5.28-MeV level is the more likely choice, since it lies below the second $J = \frac{9}{2}$ level in energy and shows a large branch to the 2.03-MeV level. Unfortunately, the lifetime of

both these levels was too fast to measure in the experiments reported here. We conclude that the strong-coupling model with band mixing is quite successful in predicting the γ-ray decay modes of the low-lying levels of Si^{29} with positive parity. The $\frac{1}{2}^+$ level at 4.84 MeV may be the band head for a $K=\frac{1}{2}$ band based on Nilsson orbit No. 11, but other members of such a band have not been identified.

C. Negative-Parity Levels and the Antianalog Level

In addition to the positive-parity levels which can be explained by the model of the previous section, one expects to find negative-parity levels based on $f_{1/2}$ and $p_{3/2}$ single-particle orbitals as well as two-particle–one-hole states among the low-lying levels of Si^{29}. Studies of the $Si^{28}(d,p)Si^{29}$ reaction have established that the $f_{7/2}$ and $p_{3/2}$ single-particle strength resides mainly in the levels at 3.62 and 4.93 MeV, respectively (Refs. 33, 9, and Table V). Our spin assignment of $\frac{3}{2}$ for the 4.93-MeV level supports this conclusion. In a previous letter[13] we discussed the decay of the $\frac{9}{2}^-$ level at 5.25 MeV to the $\frac{7}{2}^-$ level at 3.62 MeV. Since this decay shows a large collective $E2$ enhancement, and the 5.25-MeV level shows no other γ-ray branches, it appears that the 3.62- and 5.25-MeV levels might be the first two levels of a rotational band based on neutrons in Nilsson orbit No. 10. A search for the $\frac{11}{2}^-$ member of this band was unsuccessful because of the density of levels at the expected excitation energy.

The 4.90-MeV level has been identified as the antianalog of the Al^{29} ground state by Meyer-Schützmeister *et al.*[10] The identification was made on the basis of the large cross section for excitation by the $Al^{27}(He^3,p)Si^{29}$ reaction and the large $M1$ width for the decay from the analog state at 8.31 MeV to this level. The configuration is expected to be predominantly a mixture of $(2s_{1/2})^2(d_{5/2})^{-1}$ and $(d_{3/2})^2(d_{5/2})^{-1}$. The evidence from this experiment on the electromagnetic decays of this level supports its identification as the antianalog level. The $E2$ widths for decays to the first three Si^{29} levels show no collective enhancement. The $M1$ decays are also relatively weak indicating that the Si^{29} levels at 1.27 and 2.03 MeV do not contain strong admixtures of the configuration $(s_{1/2})^2(d_{5/2})^{-1}$ or $(d_{3/2})^2(d_{5/2})^{-1}$. Since one expects other levels from these configurations, these levels presumably lie above 4.9 MeV in energy.

The discussion of the preceding two sections has outlined what appears to be the predominant configuration for most of the low-lying Si^{29} levels. Eventually, it might be hoped that a comprehensive shell-model calculation such as is now beginning[58] will succeed in giving a more accurate quantitative description of the properties of these levels.

VI. ACKNOWLEDGMENTS

We wish to thank Mr. Richard Nightingale for his assistance and cooperation at several points in this experiment. He was especially helpful in connection with the computer-implemented data analysis done at Lockheed. Mrs. Diane Villar typed the manuscript with great finesse.

---

*Supported in part by the Lockheed Independent Research Fund. Work performed at the Stanford University Tandem Van de Graaff Laboratory, supported by the National Science Foundation, and at the Lockheed Nuclear Sciences Laboratory.

†Present address: Nuclear Physics Laboratory, University of Oxford, Oxford, England.

[1]A. Bohr and B. R. Mottelson, Kgl. Danske Videnskab. Selskab, Mat.-Fys. Medd. 27, No. 1 (1953).

[2]S. G. Nilsson, Kgl. Danske Videnskab. Selskab, Mat.-Fys. Medd. 29, No. 1 (1955).

[3]F. G. Bailey and D. C. Choudbury, Nucl. Phys. A144, 628 (1970).

[4]B. Castel, K. W. C. Stewart, and M. Harvey, Can. J. Phys. 48, 1490 (1970).

[5]D. A. Bromley, H. E. Gove, and A. E. Litherland, Can. J. Phys. 35, 1057 (1957).

[6]R. G. Hirko, Ph.D. dissertation, Yale University, 1969 (unpublished).

[7]J. A. Becker, L. F. Chase, Jr., and R. E. McDonald, Phys. Rev. 157, 967 (1967).

[8]A. D. W. Jones, J. A. Becker, R. E. McDonald, and A. R. Poletti, Phys. Rev. C 1, 1000 (1970).

[9]P. M. Endt and C. van der Leun, Nucl. Phys. A105, 1 (1967).

[10]L. Meyer-Schützmeister, D. S. Gemmel, R. E. Holland, F. T. Kuchnir, H. Ohnuma, and N. G. Puttaswamy, Phys. Rev. 187, 1210 (1969).

[11]A. E. Litherland, in *Nuclear Structure and Electromagnetic Interactions*, edited by N. MacDonald (Plenum, New York, 1965).

[12]E. K. Warburton, J. W. Olness, K. W. Jones, C. Chasman, R. A. Ristinen, and D. H. Wilkinson, Phys. Rev. 148, 1072 (1966); E. K. Warburton, J. W. Olness, and A. R. Poletti, *ibid.* 160, 938 (1967); P. Paul, J. B. Thomas, and S. S. Hanna, *ibid.* 147, 774 (1966). For a recent review article, see A. Z. Schwarzschild and E. K. Warburton, Ann. Rev. Nucl. Sci. 18, 265 (1968).

[13]T. T. Bardin, J. A. Becker, T. R. Fisher, and A. D. W. Jones, Phys. Rev. Letters 24, 772 (1970); T. R. Fisher, T. T. Bardin, J. A. Becker, and A. D. W. Jones, Bull. Am. Phys. Soc. 15, 600 (1970); T. T. Bardin, J. A. Becker, T. R. Fisher, and A. D. W. Jones, *ibid.* 15, 1609 (1970); T. R. Fisher, T. T. Bardin, J. A.

Becker, and A. D. W. Jones, *ibid.* 16, 58 (1971); and J. A. Becker, T. T. Bardin, T. R. Fisher, and A. D. W. Jones, *ibid.* 16, 58 (1971).

[14]Obtained from Oak Ridge National Laboratory, Stable Isotopes Division, Oak Ridge, Tennessee.

[15]Obtained from Ortec, Inc., Oak Ridge, Tennessee.

[16]P. R. Bevington, private communication.

[17]B. Watson, private communication.

[18]R. W. Nightingale, private communication.

[19]J. M. Blatt and V. F. Weisskopf, *Theoretical Nuclear Physics* (Wiley, New York, 1952).

[20]J. B. Marion, Nucl. Data A4, 301 (1968).

[21]S. Hinds and R. Middleton, quoted in R. E. White, Phys. Rev. 119, 767 (1960).

[22]E. F. Gibson, K. Battleson, and D. K. McDaniels, Phys. Rev. 172, 1004 (1968).

[23]N. Anyas-Weiss, A. M. Charlesworth, L. E. Carlson, K. P. Jackson, and R. E. Azuma, Can. J. Phys. 47, 1725 (1969).

[24]A. M. J. Spits, A. M. F. op den Kamp, and H. Gruppelaar, Nucl. Phys. A145, 449 (1970).

[25]H. Lycklama, L. B. Hughes, S. T. J. Kennett, Can. J. Phys. 45, 1871 (1967).

[26]J. K. Dickens, Phys. Rev. C 2, 990 (1970).

[27]D. C. Camp and A. L. van Lehn, Nucl. Instr. Methods 76, 192 (1969).

[28]A. E. Litherland and A. J. Ferguson, Can. J. Phys. 39, 788 (1961).

[29]E. H. Auerbach, Brookhaven National Laboratory Report No. BNL-6562 (unpublished).

[30]A. R. Poletti and E. K. Warburton, Phys. Rev. 137, B595 (1965).

[31]A. J. Ferguson, P. J. M. Smulders, T. K. Alexander, C. Broude, J. A. Kuehner, A. E. Litherland, and R. W. Ollerhead, J. Phys. Soc. Japan Suppl. 24, 1 (1968).

[32]A. A. Pilt, R. H. Spear, R. V. Elliot, and J. A. Kuehner, Bull. Am. Phys. Soc. 16, 58 (1971); Can. J. Phys. 49, 1263 (1971).

[33]M. Betigen, R. Bock, H. H. Duhm, S. Martin, and R. Stock, Z. Naturforsch 219, 980 (1966).

[34]G. Manning and G. A. Bartholomew, Phys. Rev. 115, 401 (1959).

[35]A. G. Blair and K. S. Quisenberry, Phys. Rev. 122, 869 (1961).

[36]N. V. Aleksiev, K. I. Zherebolsova, V. F. Litoin, and Yu. A. Nemilov, Zh. Eksperim. i Teor. Fiz. 39, 1508 (1960) [transl.: Soviet Phys.–JETP 12, 1049 (1961)].

[37]D. Dehnhard and J. L. Yntema, Phys. Rev. 163, 1198 (1967); Phys. Rev. C 2, 1390 (1970).

[38]R. H. Spear, J. E. Cairns, R. V. Elliot, J. A. Kuehner, and A. A. Pilt, Can. J. Phys. 49, 355 (1971).

[39]D. H. Wilkinson, in *Nuclear Spectroscopy*, edited by F. Ajzenberg-Selove (Academic, New York, 1960), Pt. B.

[40]R. W. Nightingale, R. E. McDonald, and J. A. Becker, unpublished.

[41]W. Hauser and H. Feshbach, Phys. Rev. 87, 366 (1952); E. Sheldon and D. M. van Patter, Rev. Mod. Phys. 38, 143 (1966).

[42]H. Grench *et al.*, to be published.

[43]E. K. Warburton, D. E. Alburger, and D. H. Wilkinson, Phys. Rev. 129, 2180 (1963).

[44]M. Hansen, *Constitution of Binary Alloys* (McGraw-Hill, New York, 1958), p. 214.

[45]J. Lindhard, M. Scharff, and J. E. Schiøtt, Kgl. Danske Videnskab. Selskab, Mat.-Fys. Medd. 33, No. 14 (1963).

[46]A. E. Blaugrund, Nucl. Phys. 88, 501 (1966).

[47]J. H. Ormrod and H. E. Duckworth, Can. J. Phys. 41, 1424 (1963); J. R. MacDonald, J. H. Ormrod, and H. E. Duckworth, Z. Naturforsch 21a, 130 (1966); J. H. Ormrod, J. R. MacDonald, and H. E. Duckworth, Can. J. Phys. 43, 275 (1965).

[48]S. J. Skorka, T. W. Retz-Schmidt, H. Schmidt, J. Morgenstern, and D. Evers, Nucl. Phys. 68, 177 (1965).

[49]W. M. Currie, L. G. Earwaker, and J. Martin, Nucl. Phys. A135, 325 (1969).

[50]E. K. Warburton, J. W. Olness, and A. R. Poletti, Phys. Rev. 160, 938 (1967).

[51]T. R. Fisher, S. S. Hanna, D. C. Healey, and P. Paul, Phys. Rev. 176, 1130 (1968).

[52]M. J. Wozniak, Jr., R. L. Hershberger, and D. J. Donahue, Phys. Rev. 181, 1580 (1969).

[53]S. I. Baker and R. E. Segel, Phys. Rev. 170, 1046 (1968).

[54]E. C. Booth and K. A. Wright, Nucl. Phys. 35, 472 (1962).

[55]W. Jentschke, H. J. Korner, and S. J. Skorka, Acta Phys. Austriaca 21, 43 (1966).

[56]B. Castel and K. W. C. Stewart, Phys. Rev. C 3, 964 (1971).

[57]R. G. Hirko, private communication.

[58]B. H. Wildenthal and J. B. McGrory, Bull. Am. Phys. Soc. 16, 44 (1971).